MOAI: Module-Optimizing Architecture for Non-Interactive Secure Transformer Inference

Linru Zhang[1], Xiangning Wang[1], Jun Jie Sim[2], Zhicong Huang[3], Jiahao Zhong[1], Huaxiong Wang[1], Pu Duan[2], and Kwok-Yan Lam[1]

[1]Nanyang Technological University
[2]Ant International
[3]Ant Group

October 16, 2025

Abstract

Privacy concerns have been raised in Large Language Models (LLM) inference when models are deployed in Cloud Service Providers (CSP). Homomorphic encryption (HE) offers a promising solution by enabling secure inference directly over encrypted inputs. However, the high computational overhead of HE remains a major bottleneck. To address this challenge, we propose MOAI, an efficient HE-based, non-interactive framework for secure transformer inference. MOAI gains significant efficiency improvement from: (1) a novel evaluation flow that combines column and diagonal packing with consistent strategies across all layers, eliminating expensive format conversions. (2) rotation-free algorithms for Softmax and LayerNorm that significantly reduce the number of costly HE rotations, removing 2448 HE rotations in BERT-base inference. (3) Column packing removes rotations in plaintext–ciphertext matrix multiplications and interleaved batching further reduces the rotations in ciphertext–ciphertext matrix multiplications. MOAI uses at least 1.7x fewer HE rotations compared to the state-of-the-art works across all matrix multiplications of BERT-base. As a result, We achieve a 52.8% reduction in evaluation time compared to the state-of-the-art HE-based non-interactive secure transformer inference, THOR (Moon et al., CCS'25). We then apply MOAI on the Powerformer's framework and achieve a 55.7% reduction in evaluation time compared to Powerformer (Park et al., ACL'25), which approximates Softmax and LayerNorm with simpler functions in transformer and proposes HE-based non-interactive transformer inference. We report an amortized time of 2.36 minutes per input on a single GPU environment. We show the extendibility by applying MOAI in LLaMA-3-8B. Our implementation is publicly available as open source.

1 Introduction

The Transformer architecture [30], like BERT [10], powers many NLP tasks but requires heavy computation and memory, motivating deployment on cloud service providers (CSP), which raises privacy concerns over potential data leakage. To address privacy concerns in transformer inference, prior works have explored secure multi-party computation (MPC) and fully homomorphic encryption (FHE). While MPC suffers from high communication overhead, we focus on FHE-based non-interactive inference, where the CSP performs computations directly on encrypted data and learns nothing about the user's input.

Related work. Early works [17, 23, 20] targeting interactive privacy-preserving transformer inference, usually on BERT, relied on a combination of FHE and MPC that splits the user's data into shares and distributes a share to the server.

The first non-interactive solution NEXUS, based purely on FHE, was proposed by [32] (NDSS '25). They proposed several FHE-friendly matrix multiplications and approximations for activation functions. However, NEXUS does not provide an end-to-end inference solution. NEXUS only reports performance as an aggregation of microbenchmarks. In addition, due to inconsistent packing formats, its algorithms cannot be directly composed. As also observed by [19, 22], the conversions between these formats during secure inference are not explicitly explained and the time cost of format conversions is not included in the reported performance. The state-of-the-art HE-based non-interactive solution THOR [22] (CCS'25) achieved end-to-end secure transformer inference. THOR provided inference on 128 tokens with the BERT-base model and reported 10 minutes per input on a single GPU. Format conversions are required in THOR to complete ciphertext-ciphertext matrix multiplications. NEXUS and THOR do not modify the transformer components such as Softmax and LayerNorm, and thus avoid the need for re-training or fine-tuning.

Another line of research focuses on adapting transformers to FHE-friendly functions. [34] replaced non-polynomial functions (e.g., Softmax) with polynomial alternatives. Power-Softmax [33] replaced the exponential function in Softmax with a power function and applied conventional fine-tuning. The state-of-the-art solution in this direction, Powerformer [24] (ACL'25) replaced Softmax and LayerNorm in the BERT-base model with power and linear functions, achieving 5.74 minutes per input on a single GPU. Although this line of work offers improved efficiency, it requires re-training through knowledge distillation, which limits its generalizability to other transformer architectures.

Our contributions. We focus on designing a plug-and-play FHE framework that can be seamlessly integrated into existing transformer architectures. Similar to NEXUS and THOR, we do not modify any transformer components to avoid the need for re-training through knowledge distillation.

In this paper, we present MOAI: **M**odule-**O**ptimizing **A**rchitecture for non-interactive secure transformer **I**nference. MOAI is a FHE-based. We apply MOAI

on the BERT-base model and report an amortized time of 2.36 minutes per input on a single GPU environment. We also extend our methods to decoder-only transformers, such as LLaMA-3-8B. MOAI outperforms the state-of-the-art work THOR, achieving 52.8% reduction in evaluation time in the same environment. We also show the extendibility of MOAI by applying MOAI's evaluation flow to converted FHE-friendly transformer architectures. MOAI outperforms the state-of-the-art work Powerformer, achieving 55.7% reduction in evaluation time when applying MOAI to Powerforer's FHE-friendly modifications. Our techniques can be summarized as follows:

(1) **Consistent matrix packing strategies to avoid extra format conversion.** The input ciphertexts and the evaluation of Q, K, V are in column packing. Then the output of our FHE evaluation of QK^T is in diagonal packing, which matches the input format of our FHE evaluation of Softmax. After evaluating Softmax in diagonal packing, a ciphertext - ciphertext matrix multiplication (for $\text{softmax}(QK^\intercal/\sqrt{d'})V$) takes input of one matrix encrypted in diagonal packing ($\text{Enc}(\text{softmax}(QK^\intercal/\sqrt{d'}))$) and one matrix encrypted in column packing ($\text{Enc}(V)$) and the output matrix is encrypted in column packing. Resting parts such as feedforward layers are all in column packing, and are ready to be passed to the next transformer layer without format conversion. The details of the evaluation flow is in Figure 2. Our evaluation flow ensures the consistent packing formats across all layers to avoid expensive format conversion between layers. We also remove the need of performing encrypted matrix transpose separately. In THOR, additional format conversions and transpose are necessary.

(2) **Rotation-free Softmax and LayerNorm evaluations.** Evaluating Softmax and LayerNorm in NEXUS and THOR includes a set of FHE rotations to compute a summation of data packed in a ciphertext. HE rotation is known as a computation intensive operation which affects the efficiency (e.g., [15]). We propose rotation-free Softmax and LayerNorm evaluation algorithms which eliminate rotation by putting the inputs to the summation in the same slot position of different ciphertexts. These algorithms save 2448 HE rotations in BERT-base inference.

(3) **Minimizing HE rotations in matrix multiplication.** Column packing is adopted to remove HE rotations in plaintext-ciphertext matrix multiplication. Interleaved batching is applied to further reduces the rotations in ciphertext–ciphertext matrix multiplications. MOAI achieves at least 1.7x fewer HE rotations than the state-of-the-art works across all matrix multiplications of a transformer.

2 Preliminaries

We use $[n]$ to represent the set $\{0, 1, ..., n-1\}$. We use bold lowercase letters for row vector $\mathbf{v} \in \mathbb{R}^n$ where $\mathbf{v} = [v_0, v_1, ..., v_{n-1}]$. We use $[v_i]_{i\in[n]}$ to represent the vector $\mathbf{v}$. Column vectors are represented by $\mathbf{v}^\intercal$. We define the scalar product for $c \in \mathbb{R}$ and $\mathbf{v} \in \mathbb{R}^n$, let $c\mathbf{v} = [cv_i]_{i\in[n]}$. We also define addition and Hadamard product (entry-wise multiplication) between two vectors with dimension n as

follows: $\mathbf{v}+\mathbf{u} := [v_i+u_i]_{i\in[n]}, \mathbf{v}\otimes\mathbf{u} := [v_iu_i]_{i\in[n]}$. We use $\mathrm{Rot}_k(\mathbf{v})$, for $0 \le k < n$, to denote the vector $[v_k, ..., v_{n-1}, v_0, ...v_{k-1}]$, a *left rotation* of $\mathbf{v}$. For $-n < k \le 0$, $\mathrm{Rot}_k(\mathbf{v})$ denotes a right rotation.
We use uppercase letters to denote a matrix $A \in \mathbb{R}^{m\times d}$ where $A = (a_{ij})_{i\in[m],j\in[d]}$. We use $\mathbf{a_j}^\intercal$ to represent the j-th column of A, and we can write $A = (\mathbf{a_0}^\intercal \parallel \mathbf{a_1}^\intercal \parallel \cdots \parallel \mathbf{a}_{d-1}^\intercal)$. Further, if A is a square matrix with size $m \times m$, define $\mathrm{Diag}_i(A)$ as A's i-th (upper) diagonal for $i \in [m]$: $\mathrm{Diag}_i(A) := [a_{0,i}, a_{1,i+1}, ..., a_{m-i-1,m-1}, a_{m-i,0}, ..., a_{m-1,i-1}]$.

2.1 Fully Homomorphic Encryption - CKKS Scheme

Fully Homomorphic Encryption (FHE) enables computation on encrypted data. The CKKS scheme [7] supports approximate arithmetic over complex vectors. We briefly describe CKKS and refer to Appendix H and [7] for details.

Let N be the degree of a polynomial ring, whose value is a power of 2. Q be a product of distinct primes: $Q = \prod_0^L q_i$, where L is called the *level* of the ciphertext. A fresh ciphertext starts from level L and drops to $L-1$ after a homomorphic multiplication. When remaining level is 0, decryption fails. The bootstrapping process [6] can refresh the ciphertext and restore the remaining level, enabling continued evaluations. The CKKS scheme supports SIMD-style computation by encoding $N/2$ messages into a single ciphertext, enabling parallel homomorphic operations across all slots. Let $\mathbf{v}, \mathbf{v}'$ be two vectors in $\mathbb{C}^{N/2}$ and $\mathrm{ct} = \mathrm{Enc}(\mathbf{v})$ and $\mathrm{ct}' = \mathrm{Enc}(\mathbf{v}')$. The operations supported by the CKKS scheme are as follows:

$\mathrm{Add}(\mathrm{ct}, \mathrm{ct}')$. Return a ciphertext that encrypts the vector sum $\mathbf{v} + \mathbf{v}'$.
$\mathrm{Mult}(\mathrm{ct}, \mathrm{ct}')$. Return a ciphertext that encrypts the Hadamard product $\mathbf{v} \otimes \mathbf{v}'$.
$\mathrm{PlainMult}(\mathrm{ct}, \mathbf{v}')$. Return a ciphertext that encrypts the Hadamard product $\mathbf{v} \otimes \mathbf{v}'$.
$\mathrm{Rot}_k^{\mathrm{HE}}(\mathrm{ct})$. Return a ciphertext that encrypts $\mathrm{Rot}_k(\mathbf{v}) = [v_k, ..., v_{N/2-1}, v_0, ...v_{k-1}]$.

Many previous works state that HE rotation is one of the slowest operations, and they optimize schemes by reducing the number of HE rotation (e.g., [15, 21]). Experimental results in ([31, 2]) also indicate that HE rotation performs considerably slower, especially as the ciphertext modulus increases.

2.2 Transformers and FHE-based secure transformer inference

The transformer architecture [30] follows an encoder–decoder design. We focus on the encoder (e.g., BERT), commonly used as a benchmark. Each encoder has L layers with multi-head self-attention, normalization, and feed-forward blocks. Core computations include matrix multiplication, Softmax, LayerNorm, and GELU. Further details are in Appendix A.

In FHE-based secure transformer inference, the model will take encrypted tokens as input and output encrypted results. The model is evaluated over encrypted data homomorphically, where the FHE evaluations include plaintext-ciphertext matrix multiplication (computing Q, K, V and feedforward layer),

ciphertext-ciphertext matrix multiplication (computing $QK^\intercal$ and softmax$(\cdot)V$), and non-linear evaluations such as Softmax, LayerNorm and GELU.

3 Matrix Packing, Multiplications and Interleaved Batching

3.1 Matrix Packing and multiplications

The SIMD capability of CKKS scheme allows multiple data to be packed into a single ciphertext, which offers an array-like paradigm to encode matrices for encryption. There are mainly three ways to encode an encrypted matrix in [14], namely row, column, diagonal packing. The main difficulty in designing an encrypted matrix multiplication pipeline is that the encrypted matrix must be able to fit in and switch between various forms (e.g., the transpose $A^\intercal$). To this end, we propose to use both the column packing and diagonal packing to realize seamless transition for encrypted matrix multiplication.

Definition 3.1 (Column Packing)**.** *Given a matrix $X \in \mathbb{R}^{m\times d}$, the column packing of X is a set of d CKKS ciphertexts, denoted as* $\mathrm{Enc}_{col}(X) := \left\{ \mathrm{Enc}(\mathbf{x}_0^\intercal), \mathrm{Enc}(\mathbf{x}_1^\intercal), ..., \mathrm{Enc}(\mathbf{x}_{d-1}^\intercal) \right\}$, *where $\mathbf{x_j}^\intercal$ is the j-th column of X. We say that the ciphertext of X is in* ***column packing****.*

Definition 3.2 (Diagonal Packing)**.** *Given a* ***square*** *matrix $X \in \mathbb{R}^{m\times m}$, the (upper) diagonal packing of X are m CKKS ciphertexts, denoted as* $\mathrm{Enc}_{diag}(X) := \left\{ \mathrm{Enc}(\mathrm{Diag}_0(X)), \mathrm{Enc}(\mathrm{Diag}_1(X)), ..., \mathrm{Enc}(\mathrm{Diag}_{m-1}(X)) \right\}$, *where* $\mathrm{Diag}_j(X)$ *is the j-th (upper) diagonal of X. We use* $\mathrm{Diag}_j(X)$ *as a* ***row*** *vector and say ciphertext of X is in* ***diagonal packing****.*

Encrypted matrix-vector multiplication for both packing methods were proposed in [14]. We give a brief description of the algorithms for encrypted matrix-vector multiplication for both packing methods. Let C be a square matrix of dimensions $m \times m$ and v be a vector of length m.

For column packing, denote C with its m columns as $\{\mathrm{Col}_0(C), \mathrm{Col}_1(C), ..., \mathrm{Col}_{m-1}(C)\}$. [14] first proposed an auxiliary algorithm `Replicate` that takes the vector $\mathbf{v}$ and return m-many vectors $\mathbf{v_i}$, each encrypting v_i, that is $\{\mathbf{v_i} = [v_i, v_i, \ldots, v_i]\}_{i\in[m]}$. The matrix-vector product is computed as $Cv = \sum \mathrm{Col}_i(C) \odot \mathbf{v_i}$. We can extend the matrix-vector product to matrix-matrix product by iterating over all columns of the right hand side matrix.

For diagonal packing, denote C with its m diagonals as $\{\mathrm{Diag}_0(C), \mathrm{Diag}_1(C), ..., \mathrm{Diag}_{m-1}(C)\}$. The matrix-vector product is computed as $Cv = \sum \mathrm{Diag}_i(C) \odot \mathrm{Rot}(\mathbf{v}, i)$. A subsequent improvement in [16] reduced the number of rotations needed to $O(\sqrt{m})$ by using the baby-step giant-step method (see Appendix B.1 for details).

We describe our HE matrix multiplications in both column and diagonal packing:

Case I: Calculating $\mathrm{Enc}(Q)$, $\mathrm{Enc}(K)$, $\mathrm{Enc}(V) \in \mathbb{R}^{m\times d'}$ with $\mathrm{Enc}(X)W_i + \mathbf{1}^\intercal\mathbf{b}_i$ for $i \in \{Q, K, V\}$. We encrypt X in column packing while the weights and biases are not encrypted. We note that since the weights matrices are not encrypted,

the matrix product can be interpreted as concatenations of linear combinations of X. $XW = [\sum_{i\in[d']} w_{i,0}\mathbf{x}_0^\intercal \parallel \sum_{i\in[d']} w_{i,1}\mathbf{x}_1^\intercal \parallel \cdots \parallel \sum_{i\in[d']} w_{i,d'-1}\mathbf{x}_{d'-1}^\intercal]$. The detailed algorithm is given as Algorithm 2 in Appendix B.2.

Case II: Calculating $\mathrm{Enc}(QK^\intercal)$. We remind the reader here that Q and K are encrypted in column packing as per the result of Case I. We then apply the following lemma that allows us to compute the matrix product $QK^\intercal$ where both Q and K are encrypted in column packing, without transposing K.

Lemma 3.1. *Suppose $Q, K \in \mathbb{R}^{m\times d'}$, so $QK^\intercal$ is square matrix with size $m \times m$. Then for $j \in [m]$: $\mathrm{Diag}_j(QK^\intercal) = \sum_{i=0}^{d'-1} \mathbf{q}_i \otimes Rot_j(\mathbf{k}_i)$, where $\mathbf{q}_i$ and $\mathbf{k}_i$ are the i-column of Q and K respectively.*

The result is a matrix encrypted in diagonal packing. The detailed algorithm is given as Algorithm 3 in Appendix B.2.

Case III: Calculating $\mathrm{Enc}(\mathrm{softmax}(QK^\intercal/\sqrt{d'})V)$. The encrypted matrix V is encrypted in column packing, as per Case I. For now, we briefly mention that applying the Softmax function on a diagonally packed matrix will return a diagonally packed matrix. Thus, $\mathrm{softmax}(QK^\intercal/\sqrt{d'})$ is encrypted in diagonal packing. For this matrix product, we can apply the matrix-vector product for diagonally packed matrices described earlier [14, 16] over all encrypted columns of V. The detailed algorithm is given as Algorithm 4 in Appendix B.2.

3.2 Interleaved batching

In column packing (Definition 3.1) and diagonal packing (Definition 3.2), each ciphertext encrypts a vector of dimension m, i.e., the sequence length of input. Meanwhile, the number of slots $N/2$ in the CKKS scheme is usually 2^{15}. So batching multiple vectors into one ciphertext will reduce the amortized cost. Interleaved batching, previously discussed in [3, 1] for evaluating convolutions in neural networks, is adopted in MOAI to further reduce the number of HE rotations in matrix multiplications.

Assume $m|(N/2)$. Let $N/(2m)$ vectors $\{\mathbf{x}^{(r)} \in \mathbb{R}^m\}_{r\in[N/(2m)]}$ be:

$$\mathbf{x}^{(0)} = [x_0^{(0)}, x_1^{(0)}, ..., x_{m-1}^{(0)}], ..., \mathbf{x}^{(N/(2m)-1)} = [x_0^{(N/(2m)-1)}, x_1^{(N/(2m)-1)}, ..., x_{m-1}^{(N/(2m)-1)}] ,$$

interleaved batching is defined by packing the the first entry of each vector from $\{\mathbf{x}^{(r)} \in \mathbb{R}^m\}_{r\in[N/(2m)]}$, then the second entry, and at last the last entry. We use $\tilde{\mathbf{x}} \in \mathbb{R}^{N/2}$ to represent the interleaved batching of $N/(2m)$ vectors in $\mathbb{R}^m$.

$$\tilde{\mathbf{x}} := [x_0^{(0)}, x_0^{(1)}, x_0^{(2)}, ..., x_0^{(N/(2m)-1)}, ...x_{m-1}^{(0)}, x_{m-1}^{(1)}, x_{m-1}^{(2)}, ..., x_{m-1}^{(N/(2m)-1)}] . \quad (1)$$

We use Lemma 3.2 to address the its compatibility with rotation and include its proof in Appendix C.2. The naive batching method in existing works uses two HE rotations to do one "internal rotation", which only shifts slots within each vector rather than across all slots in a ciphertext. MOAI achieves the same functionality by only one HE rotation, thereby reducing half of HE rotations.

Lemma 3.2. *Let* $\tilde{\mathbf{x}} \in \mathbb{R}^{N/2}$ *be the interleaved batching vector of* $\{\mathbf{x}^{(r)} \in \mathbb{R}^m\}_{r\in[N/(2m)]}$ *given by Eq. (1). Then* $Rot_{jN/(2m)}(\tilde{x})$ *is the interleaved batching vector of* $\{Rot_j(\mathbf{x}^{(r)})_{r\in[N/(2m)]}\}$.

Finally, we define interleaved column/diagonal packing by merging interleaved batching with our matrix packing methods directly. Please refer to Appendix C.3.

3.3 Complexity comparison

We provide a comparison of our matrix multiplications with matrix multiplications in prior FHE-based secure transformer inference works NEXUS [32](NDSS'25), THOR [22](CCS'25), and Powerformer [24](ACL'25). We focus on the total number of HE rotations, which is the most expensive underlying HE operations as discussed in Section 2.1.

In Table 1, we report the total number of HE rotations in all matrix multiplications of a transformer. [1] MOAI requires only 9648 HE rotations in all matrix multiplications in BERT model, achieving 22.9x, 2.3x, and 1.7x fewer HE rotations than NEXUS, THOR, and Powerformer, respectively.

Table 1: Comparison of number of HE rotations in matrix multiplications. For short, we use σ to denote Softmax and omit $\sqrt{d'}$. t is the intermediate size of the feed-forward layer. H is the number of heads. $c = 16$ is from THOR. $k = 64$ is from Powerformer.

Operation	Function	NEXUS #Rot^{HE}	THOR #Rot^{HE}	Powerformer #Rot^{HE}	**Our MOAI** #Rot^{HE}
Attention block	$\text{Enc}(X)W_*^{(h)}$, $*=Q,K,V$ $X\in\mathbb{R}^{m\times d}$, $W_*^{(h)}\in\mathbb{R}^{d\times d'}$, $h\in[H]$	$\frac{2md}{N/(2m)}$	$\frac{m}{2}+3(H-2)\frac{d'}{c}+\frac{3d'}{c}$	$\sqrt{\frac{5}{9}}\cdot 2\sqrt{\frac{md(3d)}{N/2}}$	0
	$\text{Enc}(Q^{(h)})\,\text{Enc}((K^{(h)})^\intercal)$ $Q^{(h)},K^{(h)}\in\mathbb{R}^{m\times d'}$	$\frac{md'H}{N/(4m)}$	$\frac{m}{2c}(\frac{m}{2}+5)+\frac{m}{2}$ $+\frac{m}{8}(\log c+3)$	$(16+14\sqrt{2})\sqrt{k}+3k$	$\frac{md'}{N/(2m)}\cdot H$
	$\text{Enc}(\sigma(\tilde{Q}^{(h)}(K^{(h)})^\intercal)\text{Enc}(V^{(h)})$ $\sigma(Q^{(h)}(K^{(h)})^\intercal)\in\mathbb{R}^{m\times m}$, $V^{(h)}\in\mathbb{R}^{m\times d'}$	N/A	$m(\log c+3)/4+m\frac{m+2}{4c}$	$(18+10\sqrt{2})\sqrt{k}+3k$	$\frac{d'(\sqrt{m}+m)}{(N/(2m))}\cdot H$
	$\text{Enc}((X^{(0)}\parallel\ldots\parallel X^{(H-1)}))W_{fc0}$ $X^{(h)}\in\mathbb{R}^{m\times d'}$, $W_{fc0}\in\mathbb{R}^{d\times d}$	$\frac{2d^2}{N/(4m)}$	$d'/2+2(H/2-1)m/c$	$\sqrt{\frac{2}{3}}\cdot 2\sqrt{\frac{md^2}{N/2}}$	0
FC1	$\text{Enc}(X)W_{fc1}$ $X\in\mathbb{R}^{m\times d}$, $W_{fc1}\in\mathbb{R}^{d\times t}$	$\frac{2md}{N/(4m)}$	$\frac{m}{2}+\frac{2t}{c}$	$\sqrt{\frac{1}{2}}\cdot 2\sqrt{\frac{mdt}{N/2}}$	0
FC2	$\text{Enc}(X)W_{fc2}$ $X\in\mathbb{R}^{m\times t}$, $W_{fc2}\in\mathbb{R}^{t\times d}$	$\frac{2mt}{N/(4m)}$	$\frac{m}{2}+\frac{2d}{c}$	$\sqrt{\frac{1}{2}}\cdot 2\sqrt{\frac{mtd}{N/2}}$	0
Total (Substitute BERT's parameters into the equation: $N=2^{16}$,$m=128$, $d=768$, $d'=64$, $H=12$, 12 layers)		>221184	22224	16740	9648

For consistency with prior work, we include a comparison if the total number of key switches in Appendix D. Key switch is the key component in the relinearization process of ciphertext multiplication and the HE rotation. MOAI requires only 834 key switches for all matrix multiplications in a single multi-head attention block, MOAI achieves the least number of key switches.

[1] 1)For NEXUS, results are taken from [32] and Table 4 in [22], and normalized by batch size. NEXUS does not specify how it evaluates the third line, so we exclude this result for NEXUS. 2)For THOR, results are taken from Table 4 in [22], include counts only from HE rotations. 3) For Powerformer, the attention block's HE rotation count in our table is computed by Algorithm 14 in [24].

4 Non-linear Function Evaluation

In this section we propose optimized evaluations of non-linear functions. Our novelty is that we do not require any rotations in evaluations of Softmax and LayerNorm. This greatly improves the speed of our algorithms. Table 2 gives a comparison between ours and NEXUS [32] (NDSS'25) and THOR [22] (CCS'25). When substitute BERT's parameters into the equation, our rotation-free Softmax and LayerNorm save 2448 HE rotations in total.

Table 2: Comparison with NEXUS [32], THOR [22] and MOAI Softmax and LayerNorm.

Function	NEXUS $\#\text{Rot}^{\text{HE}}$	THOR $\#\text{Rot}^{\text{HE}}$	**MOAI (ours)** $\#\text{Rot}^{\text{HE}}$
softmax($X \in \mathbb{R}^{m\times m}$)	$\lceil\log_2(m)\rceil \frac{m}{N/2^{\lceil\log_2(m)\rceil}}$	$\lceil\log_2(m)\rceil \frac{m}{N/2^{\lceil\log_2(m)\rceil}} \cdot 2$	**0**
LayerNorm($X \in \mathbb{R}^{m\times d}$)	$\lceil\log_2(d)\rceil \frac{d}{N/2^{\lceil\log_2(d)\rceil}}$	$\lceil\log_2(d)\rceil \frac{d}{N/2^{\lceil\log_2(d)\rceil}} \cdot 2$	**0**
Total (Substitute BERT's parameters into the equation: $N = 2^{16}$,$m = 128$, $d = 768$, $H = 12$, 12 layers)	2448	2448	**0**

Softmax. The Softmax function appears in softmax$(QK^\intercal/\sqrt{d'})V$, but we eliminate the $\sqrt{d'}$ term by folding it into W_K, saving one CKKS level. The input of Softmax is in diagonal packing, and we want the output of the Softmax function to be in diagonal packing, as the input to the next module. We introduce a novel FHE Softmax algorithm (Algorithm 1, Figure 1) that preserves this packing format and eliminates the need for rotations, based on the key insight in Lemma 4.

Lemma 4.1. *Let $C \in \mathbb{R}^{m\times m}$ be a square matrix. The summation of columns equals to the summation of diagonals: $\sum_i \mathbf{c}_i^\intercal = \sum_i \text{Diag}_i(C)$.*

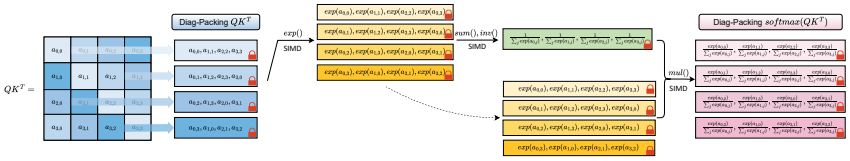

Figure 1: Our rotation-free Softmax evaluation whose input and output are both in diagonal packing.

LayerNorm. Note that the input of LayerNorm is in column packing. We first give the SIMD style mean and variance algorithm, given input as $\text{Enc}_{col}(X)$ where $X \in \mathbb{R}^{m\times d}$. For Enc$(mean(X))$, compute the summation of all encrypted columns of X and then multiply $1/d$: sMult$(1/d, \sum_i \text{Enc}(\mathbf{x}_i^\intercal))$. For Enc$(var(X))$. First compute $\text{ct}_{x^2} := \text{Mult}(\text{Enc}(\mathbf{x}_i) - \text{Enc}(mean(X)), \text{Enc}(\mathbf{x}_i) - \text{Enc}(mean(X)))$, $i \in [d]$. Then compute sMult$(1/d, \sum_{i\in[d]} \text{ct}_{x^2})$. We can merge two scalar multiplication of $1/d$ to save one FHE level. Goldschmidt division algorithm [13, 26] is applied to obtain the inverse square root $(1/\sqrt{x})$ of variance. Please refer to Algorithm 8 for the detailed explanation in Appendix E.

Algorithm 1 HE Softmax evaluation: $\mathrm{Enc}_{diag}(QK^\intercal) \to \mathrm{Enc}_{diag}(\sigma(QK^\intercal))$

Input: $\mathrm{Enc}_{diag}(QK^\intercal)$: Diagonal packing of encrypt matrix $QK^\intercal \in \mathbb{R}^{m\times m}$.
Output: $\mathrm{Enc}_{diag}(\mathrm{softmax}(QK^\intercal))$: Diagonal packing of encrypt matrix $\sigma(QK^\intercal) \in \mathbb{R}^{m\times m}$.

1: Write $\mathrm{Enc}_{diag}(QK^\intercal)$ as $\{\mathrm{Enc}(\mathrm{Diag}_0(QK^\intercal)), \mathrm{Enc}(\mathrm{Diag}_1(QK^\intercal)), ..., \mathrm{Enc}(\mathrm{Diag}_{m-1}(QK^\intercal))\}$.
2: Evaluate $\mathrm{Enc}(\exp(\mathrm{Diag}_i(QK^\intercal)))$ by SIMD polynomial evaluation $(1 + x/2^r)^{2^r}$.
3: Add ciphertexts to obtain $\mathrm{ct}_{sum} = \mathrm{Enc}(\sum_i \exp(\mathrm{Diag}_i(QK^\intercal)))$.
4: Evaluate FHE inverse algorithm on ct_{sum} using the Goldschmidt division algorithm [13]. Let the result be $\mathrm{ct}_{sum^{-1}} := \mathrm{Enc}(1/\sum_i \exp(\mathrm{Diag}_i(QK^\intercal)))$.
5: For $i \in [m]$, return $\mathrm{Mult}(\mathrm{ct}_{sum^{-1}}, \mathrm{Enc}(\exp(\mathrm{Diag}_i(QK^\intercal))))$ as the i-th component.

GELU. For the encrypted GELU algorithm using Equation 2, it suffices to approximate $\tanh(\cdot)$ function by polynomial. The main challenge is the balance between the size of effective input interval and the polynomial degree. By [8], a degree-$\Omega(R)$ polynomial is required when using minimax approximation with fixed maximum error on the domain interval $[-R, R]$. In our work, we approximate $\tanh(\cdot)$ in Equation 2 using a degree-23 polynomial $P_{23}(x)$ on interval $[-20, 10]$ which is enough in our experiment. If the model needs larger input interval, we apply the *domain extension polynomial* $B_r(x) := \frac{x}{L^r} - \frac{4}{27B^2L^{3r}}x^3$ from [8]. Let $P(x)$ be the minimax polynomial of $\tanh(x)$ on $[-B, B]$. Then $P \circ B_0(x)$ can take input from a larger interval $[-LB, LB]$ for proper L. (Theorem 4 in [8]). This can be further extended to input interval $[-L^sB, L^sB]$. We also point out that using piecewise polynomial in NEXUS [32] to approximate GELU has precision problem. Please refer to Appendix E.2 for a detailed analysis.

5 MOAI: Full Flow

The name MOAI also comes from the monolithic human figures on Easter Island. They are huge and stable. They are similar to our scheme: large and stable end-to-end inference, and with very few "rotations". We show our full diagram in Figure 2 of the BERT-base-uncased model, which is implemented and test in Section 6.1. The proposed packing flow, evaluation algorithms and interleaved batching techniques are applicable to other transformer models and even decoder-only models such as Llama3-8B.

We illustrate the dimensions and the packing formats of encrypted matrices in each module. The packing formats include column packing (Col-packing, Definition 3.1) and diagonal packing (Diag-packing, Definition 3.2). CPMM stands for ciphertext-plaintext matrix multiplication, while CCMM stands for ciphertext-ciphertext matrix multiplications. As shown in Figure 2, MOAI does not need conversion between the two packing methods.

Regarding to the number of HE rotations, Table 1 and Table 8 show that MOAI requires only 9,648 HE rotations in the full flow, yielding 23.2×, 2.56×, and 1.46× fewer HE rotations than NEXUS, THOR, and Powerformer, respectively.

Unlike Powerformer, which bypasses HE rotations by replacing Softmax and LayerNorm, MOAI preserves both and eliminates all HE rotations with rotation-free evaluation algorithms.

Figure 2: The full diagram of MOAI. The parameters are from the BERT-base-uncased model, which has 12 transformer layers and 12 heads in each layer. c is the number of classes.

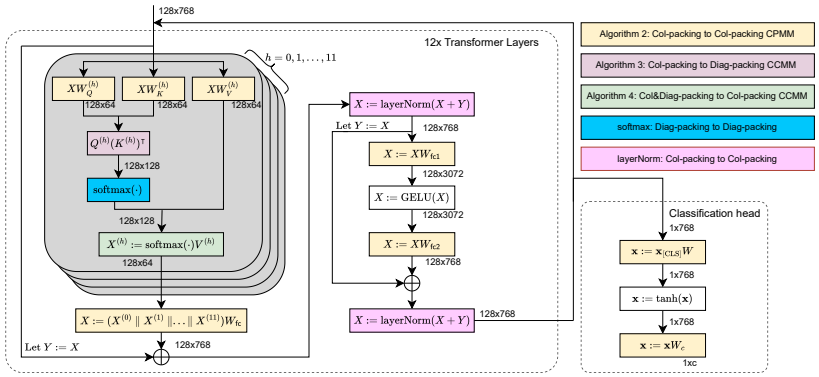

About bootstrapping. Bootstrapping is an expensive operation that resets ciphertext noise, making its placement critical for performance. We make the following two observations: (1) A sufficiently accurate Softmax requires at least 10 iterations of the Goldschmidt division (line 4 in Algorithm 1, based on experimental results in Figure 5), which together with exponentiation and final multiplication amounts to at least 20 layers (8 for e^x, 11 for division, and 1 for multiplication). (2) The runtime of matrix multiplication increases with noise level, as higher-level ciphertexts have larger moduli.

To address this, we perform bootstrapping on ct_{sum} after the third line of Algorithm 1, refreshing it before Goldschmidt division. This reduces the Softmax depth from 20 to 10 layers, allowing the two preceding matrix multiplications to be executed at a lower level. As a result, the attention block starts from lower layers, and a single bootstrapping operation on one ciphertext substantially decreases both multiplication and overall runtime. The optimized Softmax algorithm is given in Algorithm 9.

6 Experimental Results

Implementation details. We set the degree of the polynomial ring as $N = 2^{16}$, yielding 2^{15} slots in a ciphertext. We chose a 1743-bit ciphertext modulus of in accordance to the Homomorphic Encryption Standard [4] to achieve 128-bit security. We apply the scale propagation technique [5] to better manage the

noise propagation and set the scale to 2^{46} in our implementation. Our codes are available here.[2]

CPU implementation. We implement MOAI in C++, utilizing the SEAL library [29] for CKKS homomorphic encryption, FHE-MP-CNN[3] for CKKS bootstrapping, and OpenMP [9] for multi-thread programming. All CPU results are evaluated on a Intel(R) Xeon(R) Platinum 8480+ CPU at 2.0 GHz with 56 cores.

GPU implementation. MOAI is implemented using the Phantom library[4] for CKKS encryption and bootstrapping. GPU results are evaluated on a single NVIDIA H200 GPU (end-to-end evaluation in Table 3) or a single NVIDIA A100 GPU (comparison with SOTAs in Table 4 and Table 5).

Model and Dataset. Same as SOTA works THOR [22] and Powerformer [24], we test MOAI's end-to-end performance on BERT-base model. It has 12 attention heads and 12 layers with an embedding dimension of 768. The input token length is 128. In evaluations, we use the pre-trained BERT-base-uncased model fine-tuned on SST-2, QNLI, and RTE tasks.[5]

Microbenchmark. Our optimized algorithms achieve speedups of up to 22× for Softmax and 151× for LayerNorm compared to prior works. We report the microbenchmark results in Appendix G.1.

6.1 End-to-end Inference Evaluation

Table 3 presents the end-to-end performance (amortized for 256 inputs). The results are obtained from the execution of the BERT model with 12 transformer layers. For evaluating BERT model with input contains up to 128 tokens, we report an amortized time of 9.6 minutes per input on CPU and 2.36 minutes per input on GPU. Beyond encoder-only models, we extend our methods to decoder-only transformers, demonstrating them on LLaMA-3-8B inference and reporting results in Appendix G.2.

6.2 Comparison with SOTAs.

We compare MOAI with state-of-the-art works on a single NVIDIA A100 GPU, consistent with THOR [22] and Powerformer [24]. For fair comparison, we also incorporate Powerformer's pooler and classification evaluation algorithm into our packing method (column packing) to account for total evaluation time. [6]

Similar to THOR, MOAI is designed as a plug-and-play FHE framework that can be seamlessly integrated into existing transformer architectures. This

[2] CPU implementation: `https://github.com/dtc2025ag/MOAI`. GPU implementation: `https://github.com/dtc2025ag/MOAI_GPU`.

[3] https://github.com/snu-ccl/FHE-MP-CNN

[4] `https://github.com/encryptorion-lab/phantom-fhe`

[5] `https://github.com/huggingface/transformers/tree/main/examples/pytorch/text-classification`

[6] Similar to THOR and Powerformer, we do not compare end-to-end time with NEXUS [32], since it only provides microbenchmark results. Its inconsistent packing formats require costly conversions that are neither described in the paper nor implemented in its open-source code, making end-to-end reproduction infeasible (see [22, 19]).

Table 3: Breakdown of MOAI encrypted inference, amortized over 256 inputs

Component	Operation in each layer	Depth	Packing	(Data dimensions) × (Number of operations)	CPU time(s)	GPU time(s)
Attention	Pt-ct MatrixMul	$15 \to 14$	Col → Col	$(\mathbb{R}^{128\times768} \times \mathbb{R}^{768\times64}) \times 36$	37.4	10.2
	Ct-ct MatrixMul	$14 \to 13$	Col→ Diag	$(\mathbb{R}^{128\times64} \times \mathbb{R}^{64\times128}) \times 12$	40.3	8.55
	Softmax	$13 \to 3$	Diag → Diag	$\mathbb{R}^{128\times128} \times 12$	53.3	0.74
	Ct-ct MatrixMul	$3 \to 2$	Diag → Col	$(\mathbb{R}^{128\times128} \times \mathbb{R}^{128\times64}) \times 12$	1.4	0.26
Self Output	Pt-ct MatrixMul	$2 \to 1$	Col → Col	$(\mathbb{R}^{128\times768} \times \mathbb{R}^{768\times768})$	1.7	0.41
	Bootstrapping	$1 \to 21$	Col → Col	$\mathbb{R}^{128\times768}$	95.4	26.1
	LayerNorm	$21 \to 1$	Col → Col	$\mathbb{R}^{128\times768}$	0.6	0.05
	Bootstrapping	$1 \to 21 \to 10$	Col → Col	$\mathbb{R}^{128\times768}$	95.8	26.2
Intermediate	Pt-ct MatrixMul	$10 \to 9$	Col → Col	$(\mathbb{R}^{128\times768} \times \mathbb{R}^{768\times3072})$	44.1	12.7
	GELU	$9 \to 2$	Col → Col	$\mathbb{R}^{128\times3072}$	3.3	1.38
Final	Pt-ct MatrixMul	$2 \to 1$	Col → Col	$(\mathbb{R}^{128\times3072} \times \mathbb{R}^{3072\times768})$	7.1	2.5
	Bootstrapping	$1 \to 21$	Col → Col	$\mathbb{R}^{128\times768}$	98.8	26.1
	LayerNorm	$21 \to 1$	Col → Col	$\mathbb{R}^{128\times768}$	0.6	0.05
	Bootstrapping	$1 \to 21 \to 15$	Col → Col	$\mathbb{R}^{128\times768}$	94.8	26.07
Total					**574.6**	**141.3**

line of work does not modify the transformer components such as Softmax and LayerNorm, and does not need re-training or fine-tuning. Table 4 reports the layer-wise performance comparison between MOAI and THOR in the same environment with same ring dimension ($N = 2^{16}$) and slot size ($n = 2^{15}$). By reducing the number of HE rotations and adopting consistent packing strategies, MOAI achieves a 52.8% reduction in total time.

Furthermore, we apply MOAI's packing methods and evaluation algorithms to Powerformer which replaces Softmax and LayerNorm with FHE-friendly functions (BPmax and Batch LN) and retrains the model accordingly. Table 5 reports the layer-wise performance comparison between MOAI and Powerformer in the same environment, following Powerformer's parameter setting, i.e., 2^{15} slots in a ciphertext and 11 multiplicative levels before bootstrapping. MOAI achieves a 55.7% reduction in total evaluation time, demonstrating that our packing methods and evaluation algorithms can significantly improve the efficiency of retrained, FHE-friendly transformer architectures.

Operation	Ours	THOR	Diff
Attention layer	16.54	49.77	33.23
Attention score	14.07	16.25	2.18
Softmax	2.19	15.53	13.34
Attention heads	0.29	13.08	12.79
Multi-head attention	0.48	27.43	26.95
LayerNorm1	0.15	7.13	6.98
FC1	16.18	49.8	33.62
GELU	3.3	29.42	26.94
FC2	2.88	49.19	46.31
LayerNorm2	0.15	4.1	3.95
Pooler & Classification	0.7	2.7	2
Bootstrappings	227.84	337.86	110.02
Total	283.95	602.26	318.31
Total w/o Pooler & Class.	283.25	599.56	316.31

Table 4: Breakdown of execution time on a single A100 GPU compared to THOR

Operation	Ours	Powerformer	Diff
Attention layer	14.29	57.65	43.36
Attention score	6.61	28.76	22.15
BPmax	0.06	0.75	0.69
Attention heads	0.39	18.95	18.56
Multi-head attention	4.05	22.54	18.49
Batch LN1	0.004	0.37	0.366
FC1	4.79	59.21	54.42
GELU	5.2	8.31	5.83
FC2	13.79	43.77	29.98
Batch LN2	0.004	0.3	0.296
Pooler & Classification	0.7	0.2	-0.5
Bootstrappings	102.5	103.72	1.22
Total	152.4	344.52	192.12
Total w/o Pooler & Class.	151.7	344.32	192.62

Table 5: Breakdown of execution time on a single A100 GPU compared to Powerformer

6.3 Accuracy.

We analyze error propagation during encrypted evaluation by recording layer outputs and comparing them with plaintext results (Figure 3). The error grows over the first 6–7 layers but then stabilizes, indicating that it remains bounded. This shows that FHE evaluation does not cause significant accuracy loss. Further details on error variation within a layer are provided in Appendix G.3. Table 6 reports GLUE benchmark scores under both plaintext and encrypted inputs. The results indicate that the additional error introduced by FHE has only a negligible effect on inference accuracy.

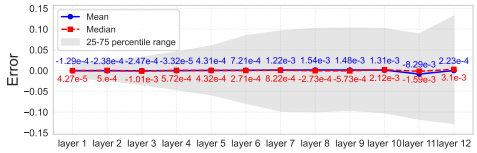

Figure 3: Error analysis of 12 layers' output

Dataset	SST-2	QNLI	RTE
Unencrypted input	93.9	90.7	65.7
Encrypted input	93.8	90.5	65.5
Match count	1818	5437	2959
Mismatch count	4	27	42

Table 6: Scores on the GLUE benchmarks

7 Conclusion

In this work, we propose MOAI, an efficient and secure transformer inference framework on encrypted data. MOAI leverages consistent matrix packing strategies, rotation-free Softmax and LayerNorm evaluations, and interleaved batching, removing format conversion, minimizing HE rotations, achieving substantial speedups and outperforming the state-of-the-art HE-based transformer inference work THOR [22](CCS'25). The proposed techniques are applicable to other revised transformer-based architectures, like Powerformer [24] (ACL'25), to speedup the secure inference time.

Acknowledgments

This work is a result of the joint lab collaboration between Ant International and Nanyang Technological University, established as part of a five-year partnership to advance digital trust and privacy-enhancing technologies (PETs), with funding provided by Ant International. This research is supported by the National Research Foundation, Singapore and Infocomm Media Development Authority under its Trust Tech Funding Initiative. Any opinions, findings and conclusions or recommendations expressed in this material are those of the author(s) and do not reflect the views of National Research Foundation, Singapore and Infocomm Media Development Authority.

References

[1] Allon Adir, Ehud Aharoni, Nir Drucker, Ronen Levy, Hayim Shaul, and Omri Soceanu. *Homomorphic Encryption for Data Science (HE4DS)*. Springer, 2024.

[2] Carlos Agulló-Domingo, Óscar Vera-López, Seyda Guzelhan, Lohit Daksha, Aymane El Jerari, Kaustubh Shivdikar, Rashmi Agrawal, David Kaeli, Ajay Joshi, and José L Abellán. Fideslib: A fully-fledged open-source fhe library for efficient ckks on gpus. In *2025 IEEE International Symposium on Performance Analysis of Systems and Software (ISPASS)*, pages 1–3. IEEE, 2025.

[3] Ehud Aharoni, Allon Adir, Moran Baruch, Nir Drucker, Gilad Ezov, Ariel Farkash, Lev Greenberg, Ramy Masalha, Guy Moshkowich, Dov Murik, et al. Helayers: A tile tensors framework for large neural networks on encrypted data. *Proceedings on Privacy Enhancing Technologies*, 2023.

[4] Martin Albrecht, Melissa Chase, Hao Chen, Jintai Ding, Shafi Goldwasser, Sergey Gorbunov, Shai Halevi, Jeffrey Hoffstein, Kim Laine, Kristin Lauter, et al. Homomorphic encryption standard. *Protecting privacy through homomorphic encryption*, pages 31–62, 2021.

[5] Jean-Philippe Bossuat, Christian Mouchet, Juan Troncoso-Pastoriza, and Jean-Pierre Hubaux. Efficient bootstrapping for approximate homomorphic encryption with non-sparse keys. In *Annual International Conference on the Theory and Applications of Cryptographic Techniques*, pages 587–617. Springer, 2021.

[6] Jung Hee Cheon, Kyoohyung Han, Andrey Kim, Miran Kim, and Yongsoo Song. Bootstrapping for approximate homomorphic encryption. In *Advances in Cryptology–EUROCRYPT 2018: 37th Annual International Conference on the Theory and Applications of Cryptographic Techniques, Tel Aviv, Israel, April 29-May 3, 2018 Proceedings, Part I 37*, pages 360–384. Springer, 2018.

[7] Jung Hee Cheon, Andrey Kim, Miran Kim, and Yongsoo Song. Homomorphic encryption for arithmetic of approximate numbers. In *International Conference on the Theory and Application of Cryptology and Information Security*, pages 409–437. Springer, 2017.

[8] Jung Hee Cheon, Wootae Kim, and Jai Hyun Park. Efficient homomorphic evaluation on large intervals. *IEEE Transactions on Information Forensics and Security*, 17:2553–2568, 2022.

[9] Leonardo Dagum and Ramesh Menon. Openmp: an industry standard api for shared-memory programming. *IEEE computational science and engineering*, 5(1):46–55, 1998.

[10] Jacob Devlin, Ming-Wei Chang, Kenton Lee, and Kristina Toutanova. Bert: Pre-training of deep bidirectional transformers for language understanding. In *Proceedings of the 2019 conference of the North American chapter of the association for computational linguistics: human language technologies, volume 1 (long and short papers)*, pages 4171–4186, 2019.

[11] Ye Dong, Wen-jie Lu, Yancheng Zheng, Haoqi Wu, Derun Zhao, Jin Tan, Zhicong Huang, Cheng Hong, Tao Wei, and Wenguang Chen. Puma: Secure inference of llama-7b in five minutes. *arXiv preprint arXiv:2307.12533*, 2023.

[12] Austin Ebel, Karthik Garimella, and Brandon Reagen. Orion: A fully homomorphic encryption framework for deep learning. In *Proceedings of the 30th ACM International Conference on Architectural Support for Programming Languages and Operating Systems, Volume 2*, pages 734–749, 2025.

[13] Robert E Goldschmidt. *Applications of division by convergence*. PhD thesis, Massachusetts Institute of Technology, 1964.

[14] Shai Halevi and Victor Shoup. Algorithms in helib. In *Annual Cryptology Conference*, pages 554–571. Springer, 2014.

[15] Shai Halevi and Victor Shoup. Faster homomorphic linear transformations in helib. In *Annual International Cryptology Conference*, pages 93–120. Springer, 2018.

[16] Shai Halevi and Victor Shoup. Bootstrapping for helib. *Journal of Cryptology*, 34(1):7, 2021.

[17] Meng Hao, Hongwei Li, Hanxiao Chen, Pengzhi Xing, Guowen Xu, and Tianwei Zhang. Iron: Private inference on transformers. *Advances in neural information processing systems*, 35:15718–15731, 2022.

[18] Dan Hendrycks and Kevin Gimpel. Gaussian error linear units (gelus). *arXiv preprint arXiv:1606.08415*, 2016.

[19] Lawrence Lim, Vikas Kalagi, Divyakant Agrawal, and Amr El Abbadi. Tricycle: Private transformer inference with tricyclic encodings. Cryptology ePrint Archive, Paper 2025/1200, 2025.

[20] Wen-jie Lu, Zhicong Huang, Zhen Gu, Jingyu Li, Jian Liu, Cheng Hong, Kui Ren, Tao Wei, and WenGuang Chen. Bumblebee: Secure two-party inference framework for large transformers. *Cryptology ePrint Archive*, 2023.

[21] Wen-jie Lu, Zhicong Huang, Cheng Hong, Yiping Ma, and Hunter Qu. Pegasus: Bridging polynomial and non-polynomial evaluations in homomorphic encryption. In *2021 IEEE Symposium on Security and Privacy (SP)*, pages 1057–1073. IEEE, 2021.

[22] Jungho Moon, Dongwoo Yoo, Xiaoqian Jiang, and Miran Kim. THOR: Secure transformer inference with homomorphic encryption. Cryptology ePrint Archive, Paper 2024/1881, 2024.

[23] Qi Pang, Jinhao Zhu, Helen Möllering, Wenting Zheng, and Thomas Schneider. Bolt: Privacy-preserving, accurate and efficient inference for transformers. In *2024 IEEE Symposium on Security and Privacy (SP)*, pages 4753–4771. IEEE, 2024.

[24] Dongjin Park, Eunsang Lee, and Joon-Woo Lee. Powerformer: Efficient and high-accuracy privacy-preserving language model with homomorphic encryption. *Cryptology ePrint Archive*, 2024.

[25] Dongjin Park, Eunsang Lee, and Joon-Woo Lee. Powerformer: Efficient privacy-preserving transformer with batch rectifier-power max function and optimized homomorphic attention. Cryptology ePrint Archive, Paper 2024/1429, 2024.

[26] Hongyuan Qu and Guangwu Xu. Improvements of homomorphic evaluation of inverse square root. *Available at SSRN 4258571*.

[27] Eugene Y Remez. Sur la détermination des polynômes d'approximation de degré donnée. *Comm. Soc. Math. Kharkov*, 10(196):41–63, 1934.

[28] Donghwan Rho, Taeseong Kim, Minje Park, Jung Woo Kim, Hyunsik Chae, Ernest K Ryu, and Jung Hee Cheon. Encryption-friendly llm architecture. *arXiv preprint arXiv:2410.02486*, 2024.

[29] Microsoft SEAL (release 4.1). `https://github.com/Microsoft/SEAL`, January 2023. Microsoft Research, Redmond, WA.

[30] Ashish Vaswani, Noam Shazeer, Niki Parmar, Jakob Uszkoreit, Llion Jones, Aidan N Gomez, Łukasz Kaiser, and Illia Polosukhin. Attention is all you need. *Advances in neural information processing systems*, 30, 2017.

[31] Hao Yang, Shiyu Shen, Wangchen Dai, Lu Zhou, Zhe Liu, and Yunlei Zhao. Phantom: A cuda-accelerated word-wise homomorphic encryption library. *IEEE Transactions on Dependable and Secure Computing*, 21(5):4895–4906, 2024.

[32] Jiawen Zhang, Xinpeng Yang, Lipeng He, Kejia Chen, Wen-jie Lu, Yinghao Wang, Xiaoyang Hou, Jian Liu, Kui Ren, and Xiaohu Yang. Secure transformer inference made non-interactive. *Cryptology ePrint Archive*, 2024.

[33] Itamar Zimerman, Allon Adir, Ehud Aharoni, Matan Avitan, Moran Baruch, Nir Drucker, Jenny Lerner, Ramy Masalha, Reut Meiri, and Omri Soceanu. Power-softmax: Towards secure llm inference over encrypted data, 2024.

[34] Itamar Zimerman, Moran Baruch, Nir Drucker, Gilad Ezov, Omri Soceanu, and Lior Wolf. Converting transformers to polynomial form for secure inference over homomorphic encryption. In *Forty-first International Conference on Machine Learning*, 2024.

A Extended Preliminaries: The BERT model

We define the mean and variance of a vector as functions from $\mathbb{R}^n \to \mathbb{R}$. We denote the softmax function and layer normalization as functions from $\mathbb{R}^n \to \{0,1\}^n$, specifically:

$$\text{softmax}(\mathbf{x}) = \left[\frac{\exp(x_i)}{\sum_{r\in[n]}\exp(x_r)}\right]_{i\in[n]} \qquad \text{LayerNorm}(\mathbf{x}) := \left[\gamma\cdot\frac{x_i - \text{mean}(\mathbf{x})}{\sqrt{\text{var}(\mathbf{x})}}+\beta\right].$$

where γ, β are model parameters. The functions softmax and LayerNorm can be directly extended to matrices, by applying the functions to each *row* of the input matrix.

Embedding. Let the input has m tokens. First it is embedded to m vectorized token embeddings, each of which has dimension d. We denote the it as matrix $X_e \in \mathbb{R}^{m\times d}$. d is also defined as the *hidden size* of the model. Let $P \in \mathbb{R}^{m\times d}$ be the positional embeddings for the input tokens. Then, the embedding input is obtained by computing $X := X_e + P$.

Multi-Head Attention. Let $X \in \mathbb{R}^{m\times d}$ be the input, $W_Q, W_K, W_V \in \mathbb{R}^{d\times d'}$ be weights matrices, and $\mathbf{b}_Q, \mathbf{b}_K, \mathbf{b}_V$ be bias vectors. An attention block in head $h \in [H]$ is defined as $\text{Attention}(Q,K,V) = \text{softmax}\left(\frac{QK^\intercal}{\sqrt{d'}}\right)V \in \mathbb{R}^{d\times d'}$, where: $Q := XW_Q + \mathbf{1}^\intercal\mathbf{b}_Q,\ K := XW_K + \mathbf{1}^\intercal\mathbf{b}_K,\ V := XW_V + \mathbf{1}^\intercal\mathbf{b}_V$. The multi-head attention is the execution of H parallel attention blocks and we set the h-th result to be $X^{(h)}$ where $d' := d/H$. Then the H matrices are concatenated $X^{\text{Concat}} := (X^{(0)} \parallel X^{(1)} \parallel ... \parallel X^{(H-1)}) \in \mathbb{R}^{m\times d}$. The attention block ends with a layer normalization procedure with a residual connection: $X := \text{LayerNorm}(X + X^{\text{Concat}})$.

Feed Forward Network. The feed forward network contains four components. A fully connected layer followed by the Gaussian Error Linear Units (GELU) [18] activation function, another fully connected layer and LayerNorm. The GELU function is defined as $\text{GELU}(x) := \frac{x}{2}\left(1 + \frac{2}{\sqrt{\pi}}\int_0^x e^{-t^2}dt\right)$. Since there is no closed-form expression for GELU, [18] suggested an approximation by tanh:

$$\text{GELU}(x) \approx 0.5x\left(1 + \tanh\left[\sqrt{2/\pi}\left(x + 0.044715x^3\right)\right]\right). \tag{2}$$

Let $W_{\mathsf{fc1}}, W_{\mathsf{fc2}}$ be weights matrices, and $\mathbf{b}_{\mathsf{fc1}}, \mathbf{b}_{\mathsf{fc2}}$ be bias vectors. The feed forward network can be described as follows: $X := \text{LayerNorm}(X + \text{GELU}(XW_{\mathsf{fc1}} + \mathbf{1}^\intercal\mathbf{b}_{\mathsf{fc1}})W_{\mathsf{fc2}} + \mathbf{1}^\intercal\mathbf{b}_{\mathsf{fc1}}) \in \mathbb{R}^{m\times d}$. The output of feed forward block is set to be the input of the attention block in the next transformer layer. The BERT-base-uncased model [10] is using $H = 12$ and it has 12 transformer layers, that is, it contains 12 attention blocks and 12 feed forward blocks.

After 12 transformer layers, the model applies a linear layer with bias and $\tanh(\cdot)$ to the first token ([CLS]) as the aggregated sequence representation for classification tasks. Let this vector be $\mathbf{x}_{[\mathrm{CLS}]} \in \mathbb{R}^d$. The classification layer first computes $\tanh(\mathbf{x}_{[\mathrm{CLS}]}W + \mathbf{1}^\intercal \mathbf{b}) \in \mathbb{R}^d$, denoted as $\mathbf{x}$. Finally let c is the number of classes, the output is $\mathbf{x}W_{\mathsf{cls}} + \mathbf{1}^\intercal \mathbf{b}_{\mathsf{cls}} \in \mathbb{R}^c$.

B Details of matrix multiplications

B.1 The baby-step-giant-step method

In [16] they optimized the algorithm by baby-step-giant-step method, and the number of HE rotations is reduced to $O(\sqrt{m})$. The idea is to write $m = g \times b$. First for $i \in [b]$, we compute $\mathrm{Rot}_i(\mathbf{v})$ for b times. To compute rotation $\mathrm{Rot}_k(\mathbf{v})$ for $k >= b$, we can write $k = \alpha b + r$ with $r < b$, and

$$\mathrm{rot}_k(\mathbf{v}) := \mathrm{rot}_{\alpha b}\big(\mathrm{rot}_r(\mathbf{v})\big) \ .$$

Combining the above, and with the diagonals of C, we will have

$$C\mathbf{v}^\intercal := \sum_{\alpha \in [g]} \mathrm{rot}_{\alpha b}\Big(\sum_{r \in [b]} \mathrm{rot}_{m-\alpha b}\big(\mathrm{Diag}_{\alpha b + r}(C)\big) \otimes \mathrm{rot}_r(\mathbf{v})\Big) \ . \tag{3}$$

B.2 Pseudo codes in Section 3

Algorithm 2 describes the detailed implementation of CPMM when X is encrypted in column packing.

Algorithm 2 Ciphertext-plaintext matrix multiplication $\mathrm{Mult}_{ct,pt}(\mathrm{Enc}_{col}(X), W, B)$.

Input: $\mathrm{Enc}_{col}(X)$: Column packing of encrypted $X \in \mathbb{R}^{m \times d}$; W: Weight matrix with size $d \times d'$. P: Bias matrix with size $m \times d'$.
Output: $\mathrm{Enc}_{col}(XW + B)$: Column packing of encrypted $XW + B \in \mathbb{R}^{m \times d'}$.

Let $Ans := \emptyset$.
Parse $\mathrm{Enc}_{col}(X)$ as $\big\{\mathrm{Enc}(\mathbf{x}_0^\intercal), \mathrm{Enc}(\mathbf{x}_1^\intercal), ..., \mathrm{Enc}(\mathbf{x}_{d-1}^\intercal)\big\}$.
for $j \in [d']$ **do**
  Let $ct_j := (0, 0) \in R_Q^2$ be a naive ciphertext.
  for $i \in [d]$ **do**
    $ct_j := \mathrm{Add}\big(ct_j, \mathrm{sMult}(w_{ij}, \mathrm{Enc}(\mathbf{x}_i^\intercal))\big)$.
  end for
  Let $\mathbf{p}_j^\intercal$ be the j-th column of P.
  $Ans := Ans \cup \mathrm{Add}(ct_j, \mathbf{p}_j^\intercal)$.
end for
Return Ans.

Algorithm 3 describes the detailed implementation for encrypted inputs. For the sake of simplicity, we assume $m = N/2$ in Algorithm 3 and 4 now. Then

the rotation of a vector with dimension m can be directly evaluated using one homomorphic rotation. When $m < N/2$ and $m|(N/2)$, [14] uses sparse packing, i.e., using m slots with index $0, N/(2m), 2 \cdot N/(2m), ..., (m-1) \cdot N/(2m)$. We will elaborate the our method of full packing in Section 3.2.

Algorithm 3 Ciphertext-ciphertext matrix multiplication: $\mathrm{Mult}_{col,col}(\mathrm{Enc}_{col}(Q), \mathrm{Enc}_{col}(K))$.

Input: $\mathrm{Enc}_{col}(Q), \mathrm{Enc}_{col}(K)$: Column packing of encrypted matrices $Q, K \in \mathbb{R}^{m \times d'}$.

Output: $\mathrm{Enc}_{diag}(QK^\intercal)$: Diagonal packing of encrypted matrix $QK^\intercal \in \mathbb{R}^{m \times m}$.

Let $Ans := \emptyset$.
Parse $\mathrm{Enc}_{col}(Q)$ as $\big\{\mathrm{Enc}(\mathbf{q}_0^\intercal), \mathrm{Enc}(\mathbf{q}_1^\intercal), ..., \mathrm{Enc}(\mathbf{q}_{d'-1}^\intercal)\big\}$.
Parse $\mathrm{Enc}_{col}(K)$ as $\big\{\mathrm{Enc}(\mathbf{k}_0^\intercal), \mathrm{Enc}(\mathbf{k}_1^\intercal), ..., \mathrm{Enc}(\mathbf{k}_{d'-1}^\intercal)\big\}$.
for $j \in [m]$ **do**
  Let $ct_j := (0,0) \in R_Q^2$ be a naive ciphertext.
  for $i \in [d']$ **do**
    if $j > 0$ **then**
      $temp := \mathrm{Rot}_j^{\mathrm{HE}}(\mathrm{Enc}(\mathbf{k}_i^\intercal))$.
    else
      $temp := \mathrm{Enc}(\mathbf{k}_i^\intercal)$
    end if
    $ct_j := \mathrm{Add}\big(ct_j, \mathrm{Mult}(\mathrm{Enc}(\mathbf{q}_i^\intercal), temp)\big)$.
  end for
  $Ans := Ans \cup ct_j$.
end for
Return Ans.

C Details of interleaved batching

C.1 Naive batching and interleaved batching

Suppose we are given $N/(2m)$ vectors $\{\mathbf{x}^{(r)} \in \mathbb{R}^m\}_{r \in [N/(2m)]}$:

$$\mathbf{x}^{(0)} = [x_0^{(0)}, x_1^{(0)}, ..., x_{m-1}^{(0)}], ..., \mathbf{x}^{(N/(2m)-1)} = [x_0^{(N/(2m)-1)}, x_1^{(N/(2m)-1)}, ..., x_{m-1}^{(N/(2m)-1)}],$$

the naive idea of batching is to arrange them one by one (e.g., in [32]):

$$\bar{\mathbf{x}} := [\mathbf{x}^{(0)}, \mathbf{x}^{(1)}, ..., \mathbf{x}^{(N/(2m)-1)}] = [x_0^{(0)}, ..., x_0^{(1)}, ..., x_0^{(N/(2m)-1)}, ..., x_{m-1}^{(N/(2m)-1)}] \in \mathbb{R}^{N/2}.$$

We call $\bar{\mathbf{x}}$ the naive batching of $N/(2m)$ vectors $\{\mathbf{x}^{(r)} \in \mathbb{R}^m\}_{r \in [N/(2m)]}$. For example, consider batching $[x_0, x_1, x_2]$ and $[y_0, y_1, y_2]$. The naive batching generates $[x_0, x_1, x_2, y_0, y_1, y_2]$, while the interleaved batching generates $[x_0, y_0, x_1, y_1, x_2, y_2]$. This naive batching method is compatible with the ciphertext-plaintext matrix

Algorithm 4 Ciphertext-ciphertext matrix multiplication: $\mathrm{Mult}_{diag,col}(\mathrm{Enc}_{diag}(C), \mathrm{Enc}_{col}(V))$.

Input: $\mathrm{Enc}_{diag}(C)$: Diagonal packing of encrypted matrices $C \in \mathbb{R}^{m\times m}$.
$\mathrm{Enc}_{col}(V)$: Column packing of encrypted matrix $V \in \mathbb{R}^{m\times d'}$.
Output: $\mathrm{Enc}_{col}(CV)$: Column packing of encrypted matrix $CV \in \mathbb{R}^{m\times d'}$.

1: Let $Ans := \emptyset$.
2: Parse $\mathrm{Enc}_{diag}(C)$ as $\big\{\mathrm{Enc}(\mathrm{Diag}_0(C)), \mathrm{Enc}(\mathrm{Diag}_1(C)), ..., \mathrm{Enc}(\mathrm{Diag}_{m-1}(C))\big\}$.
Let $c_i := \mathrm{Enc}(\mathrm{Diag}_i(C))$, for $i \in [m]$.
3: Parse $\mathrm{Enc}_{col}(V)$ as $\big\{\mathrm{Enc}(\mathbf{v}_0^\intercal), \mathrm{Enc}(\mathbf{v}_1^\intercal), ..., \mathrm{Enc}(\mathbf{v}_{d'-1}^\intercal)\big\}$.
4: Let $b := \lceil\sqrt{m}\rceil$, $g := \lceil m/b\rceil$.
5: **for** $j \in [d']$ **do**
6: **Baby step:** For $i \in [b]$, let $\beta_i := \mathrm{Rot}_i^{\mathrm{HE}}(\mathrm{Enc}(\mathbf{v}_j^\intercal))$.
7: **Giant step:** Compute the ciphertext of $C\mathbf{v}_j^\intercal$:

$$ct_j := \sum_{\alpha\in[g]} \mathrm{Rot}_{\alpha b}^{\mathrm{HE}}\Bigg(\sum_{r\in[b]} \mathrm{Mult}(\mathrm{Rot}_{m-\alpha b}^{\mathrm{HE}}(c_{\alpha b+r}), \beta_r)\Bigg) .$$

8: $Ans := Ans \cup ct_j$.
9: **end for**
10: Return Ans.

multiplication (Algorithm 2), but it is not compatible with the ciphertext-ciphertext matrix multiplications (Algorithm 3 and Algorithm 4). More concretely, this naive batching method is not compatible with rotation. When "rotate" the batched vector (e.g., Line 8 of Algorithm 3), the desired output should be a ciphertext encrypting the following "internal rotations":

$$[\mathrm{Rot}_j(\mathbf{k}^{(0)}), \mathrm{Rot}_j(\mathbf{k}^{(1)}), ..., \mathrm{Rot}_j(\mathbf{k}^{(N/(2m)-1)})] .$$

In other words, it should be rotating each $\mathbf{k}^{(i)}$ "internally", which is different from directly rotating the batched vector by $\mathrm{Rot}_j(\bar{\mathbf{k}})$. [22] proposes a method to obtain internal rotation, using 2 normal CKKS rotations and 2 plaintext-ciphertext multiplications. As a toy example, consider batching $[x_0, x_1, x_2]$ and $[y_0, y_1, y_2]$. To "internally" left rotate by 1, we should use the naive batching $\bar{\mathbf{x}} := [x_0, x_1, x_2, y_0, y_1, y_2]$ to generate $[x_1, x_2, x_0, y_1, y_2, y_0]$. This can be done by $\mathrm{Rot}_1(\bar{\mathbf{x}}) \otimes [1, 1, 0, 1, 1, 0] = [x_1, x_2, 0, y_1, y_2, 0]$. Then $\mathrm{Rot}_{-2}(\bar{\mathbf{x}}) \otimes [0, 0, 1, 0, 0, 1] = [0, 0, x_0, 0, 0, y_0]$. By summing them together we obtain $[x_1, x_2, x_0, y_1, y_2, y_0]$.

C.2 Proof of Lemma 3.2

Proof. On the one hand, by Eq. (1), we have

$$\begin{aligned}\mathrm{Rot}_{jN/(2m)}(\tilde{\mathbf{x}}) := [&x_j^{(0)}, x_j^{(1)}, x_j^{(2)}, ..., x_j^{(N/(2m)-1)},\\ &x_{j+1}^{(0)}, x_{j+1}^{(1)}, x_{j+1}^{(2)}, ..., x_{j+1}^{(N/(2m)-1)},\\ &...\\ &x_{j-1}^{(0)}, x_{j-1}^{(1)}, x_{j-1}^{(2)}, ..., x_{j-1}^{(N/(2m)-1)}] \ .\end{aligned}$$

On the other hand, $\forall r \in [N/(2m)]$, we replace $\mathbf{x}^{(r)}$ in Eq. (1) by $\mathrm{Rot}_j(\mathbf{x}^{(r)}) = [x_j^{(r)}, x_{j+1}^{(r)}, ..., x_{j-1}^{(r)}]$. Then we also obtain

$$\begin{aligned}\mathrm{Rot}_{jN/(2m)}(\tilde{\mathbf{x}}) := [&x_j^{(0)}, x_j^{(1)}, x_j^{(2)}, ..., x_j^{(N/(2m)-1)},\\ &x_{j+1}^{(0)}, x_{j+1}^{(1)}, x_{j+1}^{(2)}, ..., x_{j+1}^{(N/(2m)-1)},\\ &...\\ &x_{j-1}^{(0)}, x_{j-1}^{(1)}, x_{j-1}^{(2)}, ..., x_{j-1}^{(N/(2m)-1)}] \ .\end{aligned}$$

This finishes the proof. □

C.3 Interleaved batching for matrices

Similarly, suppose we are given $N/(2m)$ matrices $\{X^{(r)} \in \mathbb{R}^{m\times d}\}_{r\in[N/(2m)]}$. Let $\tilde{X} \in \mathbb{R}^{\frac{N}{2}\times d}$ be the *interleaved batching* matrix of $\{X^{(r)} \in \mathbb{R}^{m\times d}\}_{r\in[N/(2m)]}$. The i-th column of $\tilde{X}$ is $\tilde{\mathbf{x}}_i^\intercal \in \mathbb{R}^{N/2}$, which is the interleaved batching vector of **all** the i-th column of each $X^{(r)}$, for $r \in [N/(2m)]$, according to Eq. (1) [7]:

$$\begin{aligned}\tilde{\mathbf{x}}_i^\intercal := [&x_{i,0}^{(0)T}, x_{i,0}^{(1)T}, x_{i,0}^{(2)T}, ..., x_{i,0}^{(N/(2m)-1)T},\\ &x_{i,1}^{(0)T}, x_{i,1}^{(1)T}, x_{i,1}^{(2)T}, ..., x_{i,1}^{(N/(2m)-1)T},\\ &...\\ &x_{i,m-1}^{(0)T}, x_{i,m-1}^{(1)T}, x_{i,m-1}^{(2)T}, ..., x_{i,m-1}^{(N/(2m)-1)T}] \ .\end{aligned} \tag{4}$$

Now we are can formally define the column packing and the diagonal packing for the interleaved batching.

Definition C.1 (Column Packing for Interleaved Batching)**.** *Suppose we are given $N/(2m)$ matrices $\{X^{(r)} \in \mathbb{R}^{m\times d}\}_{r\in[N/(2m)]}$, the interleaved batching matrix of them is $\tilde{X} \in \mathbb{R}^{\frac{N}{2}\times d}$, whose i-th column is given by Eq. (4), for $i \in [d]$. Then the column packing for $\tilde{X}$ is a set of d CKKS ciphertexts, denoted as:*

$$\mathrm{Enc}_{col}(\tilde{X}) := \left\{ \mathrm{Enc}(\tilde{\mathbf{x}}_0^\intercal), \mathrm{Enc}(\tilde{\mathbf{x}}_1^\intercal), ..., \mathrm{Enc}(\tilde{\mathbf{x}}_{d-1}^\intercal) \right\} \ ,$$

where $\tilde{\mathbf{x}}_i^\intercal \in \mathbb{R}^{N/2}$ is the i-th column of $\tilde{X}$. We say that $\mathrm{Enc}_{col}(\tilde{X})$ is the ***interleaved column packing*** *of encrypted $\{X^{(r)} \in \mathbb{R}^{m\times d}\}_{r\in[N/(2m)]}$.*

[7] Here, we use $x_{i,j}^{(r)T}$ to represent the j-th entry of vector $\mathbf{x}_i^{(r)T}$.

Definition C.2 (Diagonal Packing for Interleaved Batching)**.** *Suppose we are given $N/(2m)$ square matrices $\{X^{(r)} \in \mathbb{R}^{m\times m}\}_{r\in[N/(2m)]}$. Define:*

$$\widetilde{diag}(X) := \{\widetilde{diag}(X)_i \in \mathbb{R}^{N/2}\}_{i\in[m]} \ ,$$

where $\widetilde{diag}(X)_i$ is the interleaved batching vector given by Eq. (1) using all the i-th (upper) diagonals of $X^{(r)}$, for each $r \in [N/(2m)]$. The (upper) diagonal packing of is a set of m CKKS ciphertexts, denoted as:

$$\mathrm{Enc}_{diag}(\widetilde{diag}(X)) := \left\{ \mathrm{Enc}(\widetilde{diag}(X)_0), \mathrm{Enc}(\widetilde{diag}(X)_1), ..., \mathrm{Enc}(\widetilde{diag}(X)_{m-1}) \right\} \ .$$

*We use $\widetilde{diag}(X)_i$ as a **row** vector. We say that $\mathrm{Enc}_{diag}(\widetilde{diag}(X))$ is the **interleaved diagonal packing** of encrypted $\{X^{(r)} \in \mathbb{R}^{m\times m}\}_{r\in[N/(2m)]}$.*

We conclude that the column/diagonal packing for interleaved batching is compatible with all the three homomorphic matrix multiplication algorithms (Algorithm 2, 3 and 4) using Lemma 3.2. Note that all the input and output ciphertexts of these algorithms will be encrypting the vectors in the form of the interleaved batching. Algorithm 5, 6 and 7 are the modified algorithms for homomorphic matrix multiplications using the interleaved batching.

For the HE evaluations of softmax (Algorithm 1), layer normalization (8) and GELU, we assert that the algorithm with interleaved batching input remains the same. This is because in these algorithms, the rows of the input matrix are independently evaluated. In the HE evaluations of softmax and layer normalization, if we add a permutation of rows of the input matrix, there will be the same permutation of rows of the output matrix. Note that interleaved batching is effectively a permutation of rows of the matrix. Therefore, Algorithm 1 and 8 remains the same when the input is in interleaved batching.

D Complexity Comparison

We provide a detailed comparison of the complexity of our matrix multiplications with prior FHE-based secure transformer inference works: NEXUS [32](NDSS'25), THOR [22](CCS'25), and Powerformer [24](ACL'25).

We focus on the number of key switches (KS), which refers the total count of relinearizations in ciphertext-ciphertext multiplication, rotations, conjugations and any other operations requiring a KS. The number of KS is counted in one transformer layer in the BERT-base model.

In Table 7, we provide a detailed comparison of the number of key switches required in the BERT-base model inference. For NEXUS, results are taken from [32] and Table 4 in [22], and normalized by batch size. [8] The results of THOR are from Table 4 in [22]. For Powerformer, equations are derived from Section C.2 and Algorithm 14, with numbers from Tables 11 and 12 in [24]. According to

[8] NEXUS does not specify how it evaluates $\mathrm{softmax}(Q^{(h)}(K^{(h)})^\intercal)V^{(h)}$, so we exclude this result for NEXUS.

Algorithm 5 $\mathrm{Mult}_{ct,pt}(\mathrm{Enc}_{col}(\tilde{X}), W, P)$ using interleaved batching.

Input: $\mathrm{Enc}_{col}(\tilde{X})$: Interleaved column packing of encrypted $\{X^{(r)} \in \mathbb{R}^{m\times d}\}_{r\in[N/(2m)]}$; W: Weight matrix with size $d \times d'$. P: Bias matrix with size $m \times d'$.

Output: $\mathrm{Enc}_{col}(\tilde{X}W+\tilde{P})$: Interleaved column packing of encrypted $\{X^{(r)}W + P \in \mathbb{R}^{m\times d'}\}_{r\in[N/(2m)]}$.

Let $Ans := \emptyset$.
Parse $\mathrm{Enc}_{col}(\tilde{X})$ as $\big\{\mathrm{Enc}(\tilde{\mathbf{x}}_0^\intercal), \mathrm{Enc}(\tilde{\mathbf{x}}_1^\intercal), ..., \mathrm{Enc}(\tilde{\mathbf{x}}_{d-1}^\intercal)\big\}$.
Let $\tilde{P}$ be the interleaved batching matrix of $N/(2m)$ repeated matrices P.
for $j \in [d']$ **do**
  Let $ct_j := (0,0) \in R_Q^2$ be a naive ciphertext.
  for $i \in [d]$ **do**
    $ct_j := \mathrm{Add}\big(ct_j, \mathrm{sMult}(w_{ij}, \mathrm{Enc}(\tilde{\mathbf{x}}_i^\intercal)\big)$.
  end for
  Let $\tilde{\mathbf{p}}_j^\intercal \in \mathbb{R}^{N/2}$ be j-th column of $\tilde{P}$, i.e., the interleaved batching vector of $N/(2m)$ repeated j-th column of P.
  $Ans := Ans \cup \mathrm{Add}(ct_j, \tilde{\mathbf{p}}_j^\intercal)$.
end for
Return Ans.

Algorithm 6 $\mathrm{Mult}_{col,col}(\mathrm{Enc}_{col}(\tilde{Q}), \mathrm{Enc}_{col}(\tilde{K}))$ using interleaved batching.

Input: $\mathrm{Enc}_{col}(\tilde{Q}), \mathrm{Enc}_{col}(\tilde{K})$: Interleaved column packing of encrypted $\{Q^{(r)} \in \mathbb{R}^{m\times d'}\}_{r\in[N/(2m)]}$ and encrypted $\{K^{(r)} \in \mathbb{R}^{m\times d'}\}_{r\in[N/(2m)]}$, respectively.

Output: $\mathrm{Enc}_{diag}(\widetilde{diag}(QK^\intercal))$: Interleaved diagonal packing of encrypted $\{Q^{(r)}(K^{(r)})^\intercal \in \mathbb{R}^{m\times m}\}_{r\in[N/(2m)]}$.

Let $Ans := \emptyset$.
Parse $\mathrm{Enc}_{col}(\tilde{Q})$ as $\big\{\mathrm{Enc}(\tilde{\mathbf{q}}_0^\intercal), \mathrm{Enc}(\tilde{\mathbf{q}}_1^\intercal), ..., \mathrm{Enc}(\tilde{\mathbf{q}}_{d'-1}^\intercal)\big\}$.
Parse $\mathrm{Enc}_{col}(\tilde{K})$ as $\big\{\mathrm{Enc}(\tilde{\mathbf{k}}_0^\intercal), \mathrm{Enc}(\tilde{\mathbf{k}}_1^\intercal), ..., \mathrm{Enc}(\tilde{\mathbf{k}}_{d'-1}^\intercal)\big\}$.
for $j \in [m]$ **do**
  Let $ct_j := (0,0) \in R_Q^2$ be a naive ciphertext.
  for $i \in [d']$ **do**
    if $j > 0$ **then**
      $temp := \mathrm{Rot}_{jN/(2m)}(\mathrm{Enc}(\tilde{\mathbf{k}}_i^\intercal))$.
    else
      $temp := \mathrm{Enc}(\tilde{\mathbf{k}}_i^\intercal)$
    end if
    $ct_j := \mathrm{Add}\big(ct_j, \mathrm{Mult}(\mathrm{Enc}(\tilde{\mathbf{q}}_i^\intercal), temp)\big)$.
  end for
  $Ans := Ans \cup ct_j$.
end for
Return Ans.

Algorithm 7 $\mathrm{Mult}_{diag,col}(\mathrm{Enc}_{diag}(\widetilde{diag}(C)), \mathrm{Enc}_{col}(\tilde{V}))$ using interleaved batching.

Input: $\mathrm{Enc}_{diag}(\widetilde{diag}(C))$: Interleaved diagonal packing of encrypted $\{C^{(r)} \in \mathbb{R}^{m\times m}\}_{r\in[N/(2m)]}$. $\mathrm{Enc}_{col}(\tilde{V})$: Interleaved column packing of encrypted $\{V^{(r)} \in \mathbb{R}^{m\times d'}\}_{r\in[N/(2m)]}$.

Output: $\mathrm{Enc}_{col}(\widetilde{CV})$: Interleaved column packing of encrypted $\{C^{(r)}V^{(r)} \in \mathbb{R}^{m\times d'}\}_{r\in[N/(2m)]}$.

1: Let $Ans := \emptyset$.
2: Parse $\mathrm{Enc}_{diag}(\widetilde{diag}(C))$ as $\big\{\mathrm{Enc}(\widetilde{diag}(C)_0), \mathrm{Enc}(\widetilde{diag}(C)_1), ..., \mathrm{Enc}(\widetilde{diag}(C)_{m-1})\big\}$. Let $c_i := \mathrm{Enc}(\widetilde{diag}(C)_i)$, for $i \in [m]$.
3: Parse $\mathrm{Enc}_{col}(\tilde{V})$ as $\big\{\mathrm{Enc}(\tilde{\mathbf{v}}_0^\intercal), \mathrm{Enc}(\tilde{\mathbf{v}}_1^\intercal), ..., \mathrm{Enc}(\tilde{\mathbf{v}}_{d'-1}^\intercal)\big\}$.
4: Let $b := \lceil\sqrt{m}\rceil$, $g := \lceil m/b\rceil$.
5: **for** $j \in [d']$ **do**
6: **Baby step:** For $i \in [b]$, let $\beta_i := \mathrm{Rot}iN/(2m)(\mathrm{Enc}(\tilde{\mathbf{v}}_j^\intercal))$.
7: **Giant step:** Compute the encrypted interleaved batching vector of $\{C^r(\mathbf{v}_j^{(r)})^\intercal\}_{r\in[N/(2m)]}$:

$$ct_j := \sum_{\alpha\in[g]} \mathrm{Rot}_{\alpha bN/(2m)}\Bigg(\sum_{r\in[b]} \mathrm{Mult}(\mathrm{Rot}_{(m-\alpha b)N/(2m)}(c_{\alpha b+r}), \beta_r)\Bigg).$$

8: $Ans := Ans \cup ct_j$.
9: **end for**
10: Return Ans.

Algorithm 14 in [24], Powerformer requires several BlockTrans, BlockSigma and BlockTau operations before each ciphertext–ciphertext matrix multiplication BlockMult'. All the 3 operations involve $\Theta(\sqrt{k})$ HE rotations (i.e., key switches in this case). The execution time breakdown in Table 5 further validates the results in Table 7. To evaluate all matrix multiplications in a single layer of transformer model, MOAI achieves the least number of key switches.

Table 7: Comparison of HE matrix multiplications in transformer architecture. The concrete parameters are based on BERT-base-uncased model: $m = 128$, $d = 768$, $d' = 64$, $t = 3072$, $H = 12$. N is the CKKS ring dimension. $c = 16$ is from THOR. $k = 64$ is from Powerformer.

Function	Scheme	Key switch Equation	Number
$\{XW_*^{(h)}\}_{h\in[H]}$ $X \in \mathbb{R}^{m\times d}$, $W_* \in \mathbb{R}^{d\times d'}$ $* = Q, K, V$	NEXUS	$2md/(N/(2m))$	768
	THOR	$\frac{m}{2} + 3(H-2)\frac{d'}{c} + \frac{3d'}{c}$	192
	Powerformer	$\approx \sqrt{\frac{5}{9}} \cdot 2\sqrt{\frac{md(3d)}{N/2}}$	122
	MOAI (ours)	0	**0**
$\{Q^{(h)}(K^{(h)})^\intercal\}_{h\in[H]}$ $Q^{(h)} \in \mathbb{R}^{m\times d'}$ $K^{(h)} \in \mathbb{R}^{m\times d'}$	NEXUS	$m(d'+1)H/(N/(4m))$	780
	THOR	$\frac{m}{2c}(\frac{m}{2}+7) + \frac{m}{8}(\log c + 3) + \frac{m}{2}$	460
	Powerformer	$\approx (17+14\sqrt{2})\sqrt{k} + 3k$	486
	MOAI (ours)	$((md'+m)/(N/(2m))) \cdot H$	**390**
$\{\text{softmax}(Q^{(h)}(K^{(h)})^\intercal)V^{(h)}\}_{h\in[H]}$ $\text{softmax}(Q^{(h)}(K^{(h)})^\intercal) \in \mathbb{R}^{m\times m}$ $V^{(h)} \in \mathbb{R}^{m\times d'}$	NEXUS	N/A	N/A
	THOR	$m(\log c + 3)/4 + m\frac{m+6}{4c}$	492
	Powerformer	$\approx (19+10\sqrt{2})\sqrt{k} + 3k$	457
	MOAI (ours)	$d'(\sqrt{m} + m + \sqrt{d'})/(N/(2m)) \cdot H$	**444**
$(X^{(0)} \parallel ... \parallel X^{(H-1)})W_{fc}$ $X^{(h)} \in \mathbb{R}^{m\times d'}$ $W_{fc} \in \mathbb{R}^{d\times d}$	NEXUS	$2d^2/((N/(4m)))$	9216
	THOR	$\frac{d'}{2} + 2(\frac{H}{2}-1)\frac{m}{c}$	122
	Powerformer	$\approx \sqrt{\frac{2}{3}} \cdot 2\sqrt{\frac{md^2}{N/2}}$	75
	MOAI (ours)	0	**0**
XW_{fc1} $X \in \mathbb{R}^{m\times d}$, $W_{fc1} \in \mathbb{R}^{d\times t}$	NEXUS	$(2md)/(N/(4m))$	1536
	THOR	$\frac{m}{2} + \frac{2t}{c}$	448
	Powerformer	$\approx \sqrt{\frac{1}{2}} \cdot 2\sqrt{\frac{mdt}{N/2}}$	135
	MOAI (ours)	0	**0**
XW_{fc2} $X \in \mathbb{R}^{m\times t}$, $W_{fc2} \in \mathbb{R}^{t\times d}$	NEXUS	$(2mt)/(N/(4m))$	6144
	THOR	$\frac{m}{2} + \frac{2d}{c}$	160
	Powerformer	$\approx \sqrt{\frac{1}{2}} \cdot 2\sqrt{\frac{mtd}{N/2}}$	132
	MOAI (ours)	0	**0**
Total (one transformer layer)	NEXUS	-	> 18444
	THOR	-	1874
	Powerformer	-	1407
	MOAI (ours)	-	**834**

E Details of non-linear evaluations

E.1 LayerNorm details

In this section we give the detailed implementation of LayerNorm(X). The overview of the flow is shown in Figure 4. Recall that for matrix input, LayerNorm

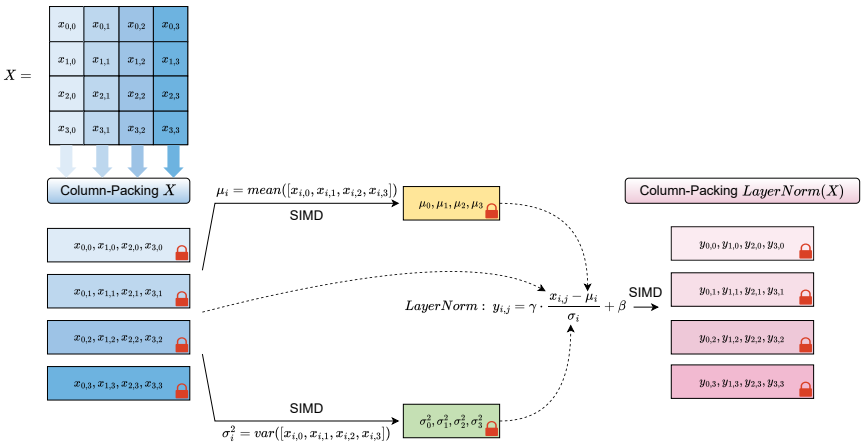

Figure 4: The flow of HE evaluation of LayerNorm.

is a "row-to-row"" function applied to each row of the input. Given one row $\mathbf{x} = [x_i]_i \in [d]$ from X, the i-th term of LayerNorm($\mathbf{x}$) is $\gamma \frac{x_i - \text{mean}(\mathbf{x})}{\sqrt{\text{var}(\mathbf{x})}} + \beta$. After computing mean() and var() we can obtain two different forms of layerNorm where $S := \sum_i x_i$:

$$\frac{\gamma}{\sqrt{d}} \frac{dx_i - S}{\sqrt{\sum_i (dx_i - S)^2 / d^2}} + \beta \ . \tag{5}$$

$$\frac{\gamma}{d} \frac{dx_i - S}{\sqrt{\sum_i (dx_i - S)^2 / d^3}} + \beta \ . \tag{6}$$

We give the detailed implementation in Algorithm 8. The parameter $t \in \{1, 2\}$ means to choose Equation 5 or Equation 6. It is for the higher precision of the inverse square root $1/\sqrt{x}$. After attention block, we choose $t = 1$ and compute LayerNorm according to Equation 5. After feed forward block, we choose $t = 2$ and compute LayerNorm according to Equation 6.

Remark. We point out the problem of the HE LayerNorm implementation of NEXUS [32]. Comparing with our Equation 5 and 6, they propose:

$$\sqrt{d}\gamma \cdot \frac{dx_i - S}{\sqrt{\sum_i (dx_i - S)^2}} + \beta \ .$$

Note that the input to the inverse square root evaluation is $\sum_i (dx_i - S)^2$, which is about $\Theta(d^3)$. In the BERT-base-uncased model $d = 768$, which makes $\sum_i (dx_i - S)^2$ extremely large and is out of the supported data range. Therefore their algorithm is unable to compute LayerNorm in BERT-base-uncased model.

Algorithm 8 HE evaluation of LayerNorm.

Input: $\mathrm{Enc}_{col}(X)$: Column packing of encrypted $X \in \mathbb{R}^{m \times d}$; model parameter $\gamma, \beta \in \mathbb{R}$; algorithm type $t \in \{1, 2\}$.

Output: $\mathrm{Enc}_{col}(\mathrm{LayerNorm}(X))$: Column packing of encrypted $\mathrm{LayerNorm}(X) \in \mathbb{R}^{m \times d}$.

Let $Ans := \emptyset$.

Parse $\mathrm{Enc}_{col}(X)$ as $\left\{ \mathrm{Enc}(\mathbf{x}_0^\intercal), \mathrm{Enc}(\mathbf{x}_1^\intercal), ..., \mathrm{Enc}(\mathbf{x}_{d-1}^\intercal) \right\}$.

Compute $\mathrm{Enc}(d \cdot \mathrm{mean}(X))$, where $\mathrm{mean}(X) \in \mathbb{R}^m$ is a vector containing the mean of each row in X:

$$\mathrm{Enc}(d \cdot \mathrm{mean}(X)) := \sum_{i \in [d]} \mathrm{Enc}(\mathbf{x}_i^\intercal) \ ,$$

i.e., the i-th element in $\mathrm{mean}(X)$ is the mean of the i-th *row* in X.

Compute $\mathrm{Enc}(d^3 \cdot \mathrm{var}(X))$, where $\mathrm{var}(X) \in \mathbb{R}^m$ is a vector containing the variance of each row in X:

for $j \in [d]$ **do**

  Compute $tmp := \mathrm{sMult}(d, \mathrm{Enc}(\mathbf{x}_i^\intercal)) - \mathrm{Enc}(d \cdot \mathrm{mean}(X))$.

  Let $tmp_j := \mathrm{Mult}(tmp, tmp)$.

end for Let $\mathrm{Enc}(d^3 \cdot \mathrm{var}(X)) = \sum_j tmp_j$.

if $t = 1$ **then**

  Compute $\mathrm{ct} := \mathrm{sMult}(\frac{1}{d^2}, \mathrm{Enc}(d^3 \cdot \mathrm{var}(X)))$.

  Use the Goldschmidt division algorithm [13, 26] to obtain the inverse square root $(1/\sqrt{x})$ of ct, denoted as ct_{sqroot}.

  Compute $\mathrm{ct}_1 := \mathrm{sMult}(\frac{\gamma}{\sqrt{d}}, \mathrm{ct}_{sqroot})$.

end if

if $t = 2$ **then**

  Compute $\mathrm{ct} := \mathrm{sMult}(\frac{1}{d^3}, \mathrm{Enc}(d^3 \cdot \mathrm{var}(X)))$.

  Use the Goldschmidt division algorithm [13, 26] to obtain the inverse square root $(1/\sqrt{x})$ of ct, denoted as ct_{sqroot}.

  Compute $\mathrm{ct}_2 := \mathrm{sMult}(\frac{\gamma}{d}, \mathrm{ct}_{sqroot})$.

end if

for $i \in [d]$ **do**

  $tmp_i := \mathrm{Mult}\left(\mathrm{ct}_t, (\mathrm{sMult}(d, \mathrm{Enc}(\mathbf{x}_i^\intercal)) - \mathrm{Enc}(d \cdot \mathrm{mean}(X)))\right) + \beta$.

  $Ans := Ans \cup tmp_i$.

end for

Return Ans.

E.2 GELU approximation

We approximate $\tanh(\cdot)$ in Equation 2 using a degree-23 polynomial $P_{23}(x)$ on interval $[-20, 10]$ which is enough in our experiment. The approximation method is the famous Remez algorithm [27]. It is noteworthy to point out that all polynomial-approximation method only support a specific interval. As suggested by [8], a degree-$\Omega(R)$ polynomial is required when using Remez or other minimax approximation with fixed maximum error on the domain interval $[-R, R]$. If the model needs larger input interval, we apply the *domain extension polynomial* $B_r(x) := \frac{x}{L^r} - \frac{4}{27B^2L^{3r}}x^3$ from [8]. In their algorithm, let $P(x)$ be the approximation polynomial of $\tanh(x)$ on $[-B, B]$. Then $P \circ B_0(x)$ can take input from a larger interval $[-LB, LB]$ for proper L. (Theorem 4 in [8]). This can be further extended to input interval $[-L^sB, L^sB]$, by using $P \circ B_{s-1} \circ ... \circ B_0(x)$.

Very recently, [28] proposed another method to control the data range. They pre-fix the desired data range of the output of each component in the transformer. Then they design punish function accordingly and perform pre-training to the model weights.

We also point out that using the piecewise polynomial in NEXUS [32] to approximate GELU has several problems. NEXUS uses a different HE evaluation of GELU which is based on the line of MPC-based solution [20, 11]. More concretely, NEXUS calculate GELU ($\mathbb{R} \to \mathbb{R}$) by the following piecewise polynomial:

$$\text{GELU}(x) := \begin{cases} 0 & x \leq -4 \\ P_3(x) & -4 < x \leq -1.95 \\ P_6(x) & -1.95 < x \leq 3 \\ x & x > 3 \end{cases} \tag{7}$$

Here $P_3(x)$ and $P_6(x)$ are polynomials with degree 3 and 6.

First, NEXUS reports the supported input range is $[-8, 8]$. We find that this range is not enough for BERT-base-uncased model, and in our experiment the range is $[-20, 10]$. Next, their piecewise polynomial relies heavily on determining which interval does the encrypted x fall in. This is done by HE evaluation of the an *approximated* sign function. For encrypted number x, NEXUS uses 4 encrypt bits $b_1(x), b_2(x), b_3(x), b_4(x)$ so that $b_i(x) = 1$ if and only if x belongs to the i-th segment of Equation 7. Ideally, $\text{GELU}(x)$ from Equation 7 can be evaluated by the following for $x \in [-8, 8]$:

$$0 \cdot b_1(x) + P_3(x)b_2(x) + P_6(x)b_3(x) + 3b_4(x) \ .$$

But in fact, each b_i are approximated bits and it is a small value ϵ instead of being 0 exactly. This will cause problems. For example, when $x = -8$, in general $P_6(-8)$ is huge, and thus $P_6(-8)b_3(-8) \approx \epsilon P_6(-8)$ is far from 0. What is more, the actually data range we observed is $[-20, 10]$, making $P_6(-20)$ extremely huge. Theoretically one can choose extreme parameters of the CKKS evaluation of sign function so that the error ϵ is small, but this will increase the time cost dramatically.

F Optimized Softmax evaluation algorithm

In this section we elaborate the optimized softmax algorithm. Figure 5 shows the error of the Goldschmidt division algorithm. Curves in different colors represent different iterations in the Goldschmidt division algorithm. The y-axis is the absolute error while the x-axis is the real data. The absolute error grows rapidly if the input data is near 0. For stable solution and higher precision, we have to ensure that input data range is not close to 0, and we need at least 10 iterations in the Goldschmidt division algorithm.

Next, at a cost of adding a bootstrapping on only one ct_{sum} after the third line of Algorithm 1, it can help to reduce the ciphertext modulus in previous matrix multiplications and can significantly reduce the time cost. The detailed optimized HE evaluation of softmax is shown in Algorithm 9.

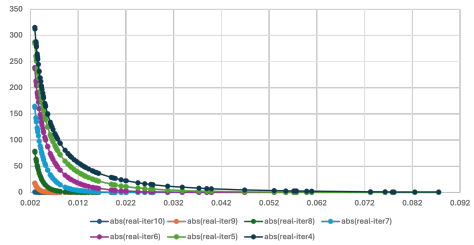

(a) Absolute error of Goldschmidt division algorithm in Softmax

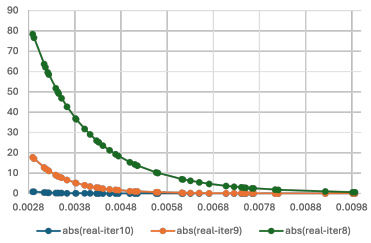

(b) Details of the bottom left corner of the figure

Figure 5: Absolute error of Goldschmidt division algorithm in Softmax

Algorithm 9 HE Softmax evaluation: $\mathrm{Enc}_{diag}(QK^\intercal) \to \mathrm{Enc}_{diag}(\sigma(QK^\intercal))$

Input: $\mathrm{Enc}_{diag}(QK^\intercal)$: Diagonal packing of encrypt matrix $QK^\intercal \in \mathbb{R}^{m\times m}$.
Output: $\mathrm{Enc}_{diag}(\mathrm{softmax}(QK^\intercal))$: Diagonal packing of encrypt matrix $\sigma(QK^\intercal) \in \mathbb{R}^{m\times m}$.

1: Write $\mathrm{Enc}_{diag}(QK^\intercal)$ as $\{\mathrm{Enc}(\mathrm{Diag}_0(QK^\intercal)), \mathrm{Enc}(\mathrm{Diag}_1(QK^\intercal)), ..., \mathrm{Enc}(\mathrm{Diag}_{m-1}(QK^\intercal))\}$.
2: Evaluate $\mathrm{Enc}(\exp(\mathrm{Diag}_i(QK^\intercal)))$ by SIMD polynomial evaluation $(1 + x/2^r)^{2^r}$.
3: Add ciphertexts to obtain $\mathrm{ct}_{sum} = \mathrm{Enc}(\sum_i \exp(\mathrm{Diag}_i(QK^\intercal)))$.
4: Bootstrap ct_{sum} to obtain refreshed ciphertext $\mathrm{ct}'_{sum} = \mathrm{Enc}(\sum_i \exp(\mathrm{Diag}_i(QK^\intercal)))$
5: Evaluate HE inverse algorithm on ct'_{sum} using the Goldschmidt division algorithm [13]. Let the result be $\mathrm{ct}'_{sum^{-1}} := \mathrm{Enc}(1/\sum_i \exp(\mathrm{Diag}_i(QK^\intercal)))$.
6: For $i \in [m]$, return $\mathrm{Mult}(\mathrm{ct}'_{sum^{-1}}, \mathrm{Enc}(\exp(\mathrm{Diag}_i(QK^\intercal))))$ as the i-th component.

G Details of experimental results

G.1 Micro-benchmark evaluation of Softmax and LayerNorm

We compare our implementation of rotation-free SoftMax and LayerNorm evaluation algorithms with NEXUS [32] (NDSS'25) and THOR [25] (CCS'25).

All experiments are evaluated with same polynomial ring dimension ($N = 2^{16}$) and slot size ($n = 2^{15}$). All CPU experiments are conducted on an Intel(R) Xeon(R) Platinum 8480+ processor using a single-thread setting, and all GPU experiments are performed on a single NVIDIA A100 GPU. We evaluate NEXUS using its open-source implementation[9], invoking its SoftMax and LayerNorm modules in both CPU and GPU environments. In contrast, THOR does not provide an open-source CPU implementation nor report CPU results; therefore, only GPU timings are included for THOR.

The amortized time taken for both functions are given in Table 8. By eliminating all rotations during evaluation, our SoftMax evaluation algorithm achieves at least 4× speedup over NEXUS and 22× over THOR, while our LayerNorm evaluation algorithm achieves at least 87× and 151× speedup, respectively.

Table 8: Comparison between Softmax and LayerNorm implementations

Scheme	Softmax			LayerNorm		
	Size	CPU time(s)	GPU time(s)	Size	CPU time(s)	GPU time(s)
MOAI	128×128	**0.62**	**0.005**	128×768	**0.38**	**0.0039**
NEXUS (NDSS'25)	128×128	2.53	0.032	128×768	46.7	0.34
THOR (CCS'25)	128×128	-	0.11	128×768	-	0.59

G.2 Inference time on Llama3-8B model

In this section, we apply our methods in LLaMA-3-8B model. LLaMA-3-8B is a 32-layer decoder-only Transformer with 4096 hidden size, 32 attention heads (grouped-query attention), a feed-forward dimension of 14,336 (SwiGLU), RoPE positional embeddings, RMSNorm normalization, and a vocabulary size of 128k tokens.

To evaluate LLaMA-3-8B model, we implement rotation-free softmax with a causal mask and RMSNorm evaluations by using the same idea of rotation-free SoftMax and LayerNorm evaluations. SiLU evaluation, similar to GELU evaluation, uses a polynomial to approximate it according to [12]. We incorporate NEXUS's ArgMax evaluation algorithm [32] into MOAI to measure total evaluation time. In the extract-token step, we retain only the last token and repack multiple ciphertexts into one, producing row-packed ciphertexts consistent with NEXUS's ArgMax evaluation. The results in Table 9 aggregate microbenchmarks that cover all components required for LLaMA-3-8B inference. The matrix packing strategies remain consistent, without requiring format conversions or

[9] `https://github.com/zju-abclab/NEXUS`

transpositions. We use 8-token input for consistency with PUMA [11] and NEXUS [32]. Note that comparing our results with NEXUS is not appropriate because: (1) NEXUS's inconsistent packing formats require costly conversions, which are not reflected in its reported performance, as observed in [22, 19]; and (2) NEXUS does not implement all LLaMA-3-8B components, such as RoPE and SwiGLU.

Table 9: Amortized breakdown of MOAI encrypted inference of LLaMA-3-8B with 8 input tokens

Operation in each layer	Description	Depth	(Data dimensions) × (Number of operations)	GPU time(s)
Pt-ct MatrixMul	$Q = XW_Q$	$17 \to 16$	$(\mathbb{R}^{8\times 4096} \times \mathbb{R}^{4096\times 4096})$	20.2
Pt-ct MatrixMul	$K = XW_K$, $V = XW_V$	$17 \to 16$	$(\mathbb{R}^{8\times 4096} \times \mathbb{R}^{4096\times 1024}) \times 2$	10.1
Pt-ct position-wise Mul	RoPE(Q)	$16 \to 15$	$(\mathbb{R}^{8\times 8} \times \mathbb{R}^{8\times 8}) \times 32$	0.11
Pt-ct position-wise Mul	RoPE(K)	$16 \to 15$	$(\mathbb{R}^{8\times 8} \times \mathbb{R}^{8\times 8}) \times 8$	0.025
Ct-ct MatrixMul	$QK^\intercal$	$15 \to 14$	$(\mathbb{R}^{8\times 8} \times \mathbb{R}^{8\times 8}) \times 32$	8.6
Casual masked SoftMax	$\sigma'(QK^\intercal)$	$14 \to 3$	$\mathbb{R}^{8\times 8} \times 32$	0.6
Ct-ct MatrixMul	$\sigma'(QK^\intercal)V$	$3 \to 2$	$(\mathbb{R}^{8\times 8} \times \mathbb{R}^{8\times 8}) \times 32$	0.2
Pt-ct MatrixMul	$XW_{\text{selfoutput}}$	$2 \to 1$	$(\mathbb{R}^{8\times 4096} \times \mathbb{R}^{4096\times 4096})$	1.3
Bootstrapping	-	$1 \to 20$	$\mathbb{R}^{8\times 4096}$	8.8
RMSNorm	Normalization	$20 \to 1$	$\mathbb{R}^{8\times 4096}$	0.06
Bootstrapping	-	$1 \to 20 \to 14$	$\mathbb{R}^{8\times 4096}$	8.8
Pt-ct MatrixMul	$u = XW_u, v = XW_v$	$14 \to 13$	$(\mathbb{R}^{8\times 4096} \times \mathbb{R}^{4096\times 14336}) \times 2$	97.8
SiLU	$h = \text{SiLU}(u)$	$13 \to 3$	$\mathbb{R}^{8\times 14336}$	6.5
Position-wise Mul	$h = h \odot v$	$3 \to 2$	$\mathbb{R}^{8\times 14336}$	0.02
Pt-ct MatrixMul	$y = hW_o$	$2 \to 1$	$(\mathbb{R}^{8\times 14336} \times \mathbb{R}^{14336\times 4096})$	48.8
Bootstrapping	-	$1 \to 21$	$\mathbb{R}^{8\times 4096}$	8.7
RMSNorm	Only in the last layer	$21 \to 2$	$\mathbb{R}^{8\times 4096}$	0.001
Extract token	Only in the last layer	$2 \to 1$	$(\mathbb{R}^{8\times 4096} \to \mathbb{R}^{1\times 4096})$	0.07
Bootstrapping	Only in the last layer	$1 \to 21 \to 2$	$\mathbb{R}^{1\times 4096}$	0.015
Pt-ct Matrix-vector Mul	Only in the last layer	$2 \to 1$	$(\mathbb{R}^{1\times 4096} \times \mathbb{R}^{4096\times 128256})$	0.86
Bootstrapping	Only in the last layer	$1 \to 21 \to 11$	$\mathbb{R}^{1\times 128256}$	0.47
ArgMax	Only in the last layer	$11 \to 1$	$\mathbb{R}^{128256}$	2.5
Total				224.53

G.3 Error analysis in one transformer layer

We divide one transformer layer into 4 parts: (1) Row 1 to Row 4 in Table 3. We call it attention layer; (2) Row 5 to Row 8 in Table 3. We call it self-output layer; (3) Row 9 to Row 10 in Table 3. We call it intermediate layer; (4) Row 11 to Row 14 in Table 3. We call it final output layer.

Figure 6 illustrated the absolute errors of evaluating the first layer with 44 input tokens. It shows that the error grows slowly along the evaluation and the medians of them fall into $[0.01, 0.03]$ in the final output of the layer, which is consistent with our error analysis of evaluating 12 layers.

H Set up operations of the CKKS scheme

Finally, we give more details of the CKKS scheme [7, 6]. The set up, encryption and decryption of the CKKS scheme can be summerized as follows.

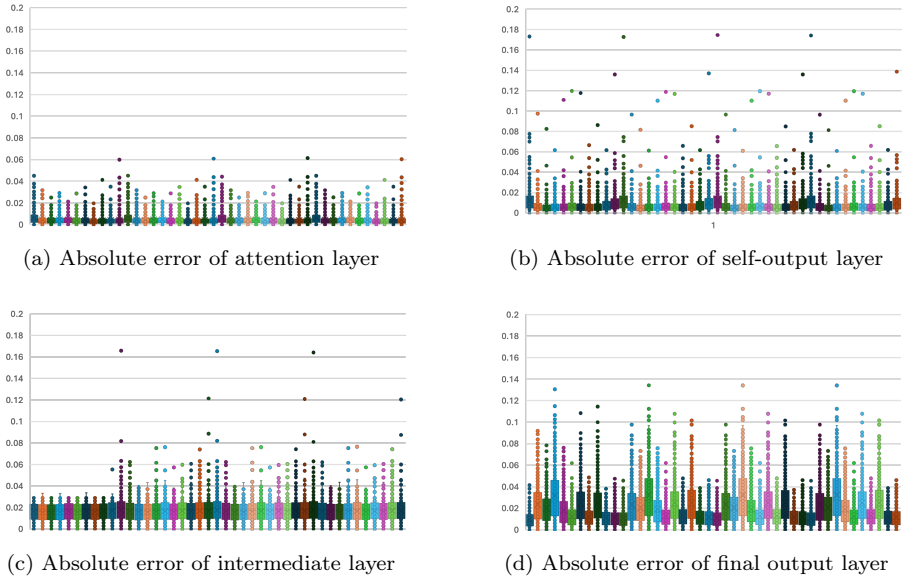

(a) Absolute error of attention layer

(b) Absolute error of self-output layer

(c) Absolute error of intermediate layer

(d) Absolute error of final output layer

Figure 6: Box and whisker figure of absolute error in one layer

- $Setup(1^\lambda)$. The input is a security parameter λ. The output is a parameter set *parms* of the scheme, including the ciphertext modulus Q, and polynomial degree N.
- $KeyGen(parms)$. The output includes secret key sk, public key pk and other auxiliary data called evaluation keys.
- $\text{Enc}_{\text{pk}}(\mathbf{v})$. Given the vector $\mathbf{v} \in \mathbb{C}^{N/2}$, the output ciphertext is $\text{ct} := (a, b) \in R_Q^2$. For convenience, we will use $\text{Enc}(\mathbf{v})$ when the public key is clear from context. We will use *naive ciphertext* to refer to $(0, 0) \in R_Q^2$ which is a ciphertext of $\mathbf{0}$.
- $\text{Dec}_{\text{sk}}(\text{ct})$. It outputs the vector $\mathbf{v} \in \mathbb{C}^{N/2}$. sk is omitted when it is clear from context.